

NPS ARCHIVE
1965
VAUGHAN, E.

AN INVESTIGATION INTO ONE METHOD
OF OBTAINING ACCURATE BEARING RATES
FROM PASSIVE SONAR BEARINGS

EDWARD BRESSIE VAUGHAN, JR.

DUDLEY KNOX LIBRARY
NAVAL POSTGRADUATE SCHOOL
MONTEREY CA 93943-5101

AN INVESTIGATION INTO ONE METHOD
OF OBTAINING ACCURATE BEARING
RATES FROM PASSIVE SONAR BEARINGS

* * * * *

Edward Bressie Vaughan, Jr.

AN INVESTIGATION INTO ONE METHOD
OF OBTAINING ACCURATE BEARING
RATES FROM PASSIVE SONAR BEARINGS

by

Edward Bressie Vaughan, Jr.
Lieutenant, United States Navy

Submitted in partial fulfillment of
the requirements for the degree of

MASTER OF SCIENCE

IN

ELECTRICAL ENGINEERING

United States Naval Postgraduate School
Monterey, California

1 9 6 5

1965

Vaughan, E.

AN INVESTIGATION INTO ONE METHOD
OF OBTAINING ACCURATE BEARING
RATES FROM PASSIVE SONAR BEARINGS

by

Edward Bressie Vaughan, Jr.

This work is accepted as fulfilling
the thesis requirements for the degree of

MASTER OF SCIENCE

IN

ELECTRICAL ENGINEERING

from the

United States Naval Postgraduate School

ABSTRACT

The need for a device capable of measuring bearing rate is shown. Some specifications for such a device are set forth. Several possible means of obtaining bearing rate from continuous passive sonar bearings are then considered. The feasibility of one of these means is then studied in detail through the development of an "initial" and then a "final" prototype. A conclusion is reached that the "final" device as constructed performs adequately. Several recommendations for improvement of this "final" device are suggested.

ACKNOWLEDGEMENTS

The author wishes to express his appreciation for the advice and encouragement shown him by Professor Milton L. Wilcox of the U. S. Naval Postgraduate School in this investigation of a bearing rate measuring device.

Appreciation is also extended to Mr. Allen J. White, Mr. John Yarnell, and Mr. Shirley Daman of the Department of Electrical Engineering at the U. S. Naval Postgraduate School for frequent practical advice and assistance in constructing the prototype devices. Mr. Michael O'Day and Mr. Norman Walker of the Machine Shop Facility of the U. S. Naval Postgraduate School rendered invaluable aid in constructing the precision gear train which was used in the final prototype device.

Special appreciation is expressed for one corporation which rendered a most significant assistance. This was the Librascope Group of General Precision Inc. Librascope made the only offer to provide an amplifier on a loan basis. Particular appreciation is expressed to Mr. Richard A. Potter of Librascope who made many valuable suggestions for development of the device.

TABLE OF CONTENTS

Section	Title	Page
1.	Introduction	1
	1.1 Purpose	1
	1.2 Organization	1
2.	Background	2
	2.1 Necessity for Accurate Bearing Rates	2
	2.2 Device Requirements	3
3.	Possible Methods of Obtaining Bearing Rate from Continuous Passive Sonar Bearings	5
	3.1 Electrical Differentiation Device, Type I	5
	3.2 Position Servo Loop Operation	8
	3.3 Electronic Counter Device	9
	3.4 Eddy Current Device	11
	3.5 Galvanometer Device, Type A	11
	3.6 Galvanometer Device, Type B	16
	3.7 Gyroscopic Precession Device	16
	3.8 Choice of Type Device to be Tested	18
4.	Development of Initial Prototype Bearing Rate Device	20
	4.1 Description of Initial Prototype Device	20
	4.2 Obtaining Constants from Initial Prototype Device	23
	4.3 Bearing Rate Device Feasibility	35
5.	Development of Final Prototype Device	41
	5.1 Final Prototype Servo Loop	41
	5.2 Bearing Rate Meter	47
	5.3 Isolation of Tachometer	48
	5.4 Device Test Equipment	48

Table of Contents (Cont'd)

Section	Title	Page
5.5	Testing of Final Prototype Device and Components	50
5.6	Bearing Rate Meter Calibration	55
5.7	Test Results for Final Prototype Device	55
6.	Recommendation for Additional Development and Conclusion	58
6.1	Recommendation for Additional Development	58
6.2	Conclusion	58
	Bibliography	59
Appendix A	Initial Prototype Device Computer Programs	60
Appendix B	Initial Prototype Device	62

LIST OF ILLUSTRATIONS

Figure		Page
3-1	Synchro Voltage vs. Time	5
3-2	Half-wave Rectifier and Holding Circuit	6
3-3	Output of Half-wave Rectifier and Holding Circuit vs. Time	6
3-4	Synchro Voltage vs. Bearing	7
3-6	Electronic Counter Device, Schematic Diagram	10
3-7	Eddy Current Device, Schematic Diagram	12
3-8	Servo Loop Block Diagram	14
3-9	Typical Appearance of Sonar Bearing vs. Time	15
4-1	Initial Prototype Device, Schematic Diagram	21
4-2	Initial Prototype Device Servo Amplifier, Circuit Diagram	22
4-3	Initial Prototype Device Gear Train	25
4-4	Initial Prototype Device Block Diagram	31
4-5	Initial Prototype Device Program Analog Block Diagram	32
4-6	Initial Prototype Device Analog Computer Simulation	33
4-7	Initial Prototype Device Bode Diagram, $K_e = 10$ $K_t = 10$	36
4-8	Initial Prototype Device Bode Diagram, $K_e = 100$ $K_t = 10$	37
4-9	Initial Prototype Device Bode Diagram, $K_e = 10$ $K_t = 100$	38
4-10	Initial Prototype Device Bode Diagram, $K_e = 100$ $K_t = 100$	39
4-11	Initial Prototype Device Steady State Tachometer Voltage vs. Bearing Rate	40
5-1	Final Prototype Device Servo Amplifier Circuit Diagram, BUORD Drawing # 1836748	43
5-2	Servo Amplifier Input Network BUORD Drawing # 207521	44
5-3	Final Prototype Gear Train	45
5-4	Simpson Compensated Wattmeter Schematic Diagram	47

List of Illustrations (Cont'd)

Figure		Page
5-5	Trutone Electronics Audio Amplifier, Model 904, Circuit Diagram	49
5-6	Bearing Rate Generation Gear Train	51
5-7	Bearing Rate and Noise Generation System	52
5-8	Bearing Rate Wattmeter as Partially Compensated	56
B-1	Tachometer Output Voltage vs. Tachometer Speed for Initial Prototype Device	64
B-2	Retardation Test, Tachometer Voltage vs. Time	65
B-3	Servo Amplifier Tachometer Channel Gain Curve	67
B-4	Servo Amplifier Error Channel Gain Curve	68
B-5	Servo Amplifier Gain Curve	69
B-6	Control Transformer Sensitivity Curve	70

LIST OF TABLES

Table		Page
4-1	Initial Prototype Gear and Shaft Moments of Inertia	26
4-2	Motor, Tachometer, and Control Transformer Data for Initial Prototype	27
4-3	Gear Ratio Data	28
4-4	Constants and Parameters for Initial Prototype Device	30
5-1	Typical Bearing Rates and Noise	54
B-1	Tachometer Calibration Data	63
B-2	Tachometer Channel Gain Data	71
B-3	Error Channel Gain Data	72
B-4	Amplifier Gain Data	73
B-5	Control Transformer Sensitivity	74

TABLE OF SYMBOLS AND ABBREVIATIONS

Symbol	Definition
a.c.	Alternating current
A	Gain of servo amplifier
B	Bearing
\dot{B}_r	Bearing rate
cm	Centimeter
DB	Decibel
d.c.	Direct current
E	Control Transformer error voltage
f	Friction of the rotating components as referred to the motor shaft
gm	Gram
J	Inertia of all rotating components referred to the motor shaft
k_s	Synchro control transformer sensitivity
K_e	Error channel potentiometer setting
K_t	Tachometer channel potentiometer setting
ms	Millisecond
r	ripple factor
ms	root mean square
s	Laplace transformer operator
sec	second
t	Time
(t)	A function of time
T_M	Torque used by the motor
T_{LOAD}	Torque used by the load
V_t	Tachometer output voltage

Table of Symbols and Abbreviations (Cont'd)

Symbol	Definition
θ_c	Servo loop follow up bearing
θ_r	Target bearing (electrical or mechanical)
θ_m	Motor angular position
$\dot{\theta}_m$	Motor angular velocity
$\ddot{\theta}_m$	Motor angular acceleration

SECTION I

1. Introduction

1.1 Purpose

There exist several possible means by which accurate bearing rate may be obtained from continuous passive sonar bearings. Bearing rate is the first time derivative of bearing that is:

$$\dot{B}_r = \frac{d}{dt} (B_r)$$

It is the objective of this report to consider several methods by which bearing rate might be obtained from continuous passive sonar bearings; to determine which possible method offers promise of success coupled with reliability, ruggedness, and reasonable cost; and finally to actually develop and test a prototype of such a device.

1.2 Organization

This report will be organized into six major parts. The first of these is the background or justification for the requirement for a device which can give bearing rate and selection of basic requirements for the device. The second major part is a brief investigation into several of the methods by which bearing rate might be obtained from continuous passive sonar bearings and the choosing of the method to be utilized for the prototype device. The next two sections give the development and testing of an initial prototype and then final prototype bearing rate device. The final two sections relate to the performance of the type device tested and recommendations regarding utilization and/or continued development of the type bearing rate device selected.

SECTION 2

2. Background

2.1 Necessity for Accurate Bearing Rates

It is well known that submarines are among the major weapons delivery devices of the United States Navy. Accurate and rapid solution of the torpedo fire control problem for the friendly submarine vs. an enemy surface ship or submarine by information obtained from passive sonar bearings has long been an area which left room for improvement. A major part of the solution of this fire control problem involves determination of the course, speed, and range of the target vessel. Present methods of solution of the problem often accept target speed as an assumed factor from information regarding turns per knot intelligence and target identification by experienced sonar operators. Given target speed and the bearing rates at several bearings target range and course can be determined. Methods also exist whereby the target may be accurately determined from bearing rate vs. bearing information. Accuracy of the torpedo fire control problem solution using only passive sonar information is directly dependent upon the accuracy of bearing rate determination.

Present methods for the obtaining of bearing rate involve manual plotting, "fairing" the bearings in order to obtain an approximation of a least squares fit, and manipulation of a device so that bearing rate may be visually determined. "Fairing" is nothing but visual smoothing of bearings plotted at discrete time intervals. Practice and teamwork of two or more individuals is required in order to accomplish this with even a fair amount of accuracy. The necessity for "faired bearings" often results in an unacceptable time delay in bearing rate determination of as much as three or four minutes. In

Addition to this very high bearing rates are difficult to determine due to inability to maintain the plots required.

Present torpedo firing doctrine frequently calls for the launching of a "spread" of more than one sophisticated and very expensive homing torpedoes at an enemy. There exists a pronounced possibility that with better bearing rate information a more accurate up to date torpedo fire control solution can be regularly obtained. This offers the promise of a potential change in torpedo firing doctrine whereby there will be used "one torpedo for one target." Aside from the pecuniary advantages obtained by more economic torpedo utilization, a pronounced advantage is obtained in wartime because a submarine has the ability to engage more targets before expending all weapons. The potential advantages which are offered by up to date accurate bearing rates more than justify the time, effort, and funds used in this investigation.

2.2 Device Requirements

Based on the operational experience of this writer and that of several other naval officers who are also designated as "qualified in submarines," there are several desirable features that should be incorporated into the device to be tested. Not restricted to but included in the device are:

- a) Operation should be simple
- b) The device should be inexpensive
- c) The device should be compatible with existing passive sonars and bearing transmission systems
- d) Accuracy of the bearing rate should be $\pm .05$ degrees per minute or $\pm 1\%$, whichever is larger
- e) Bearing rates between 0 and 100 degrees per minute right or left should be able to be measured

- f) The unit should have a small size, certainly no more than 1.5 cubic feet
- g) The device should be capable of being installed by ships personnel, thereby avoiding the necessity of having to go to a navy yard for installation
- h) Like all equipment aboard warships, the device should be rugged and capable of resisting physical shock

SECTION 3

3. Possible Methods of Obtaining Bearing Rate from Continuous Passive Sonar Bearings

There exist several possible methods which can conceivably be used to obtain bearing rates from passive sonar synchro bearings. Without resorting to expensive and very complex systems, these methods include:

3.1 Electrical Differentiation, Type 1

Electrical differentiation of a rectified sonar synchro bearing voltage signal is one possible means of obtaining bearing rate. The synchro voltage can be thought of as an amplitude modulated wave such as is shown in figure 3-1.

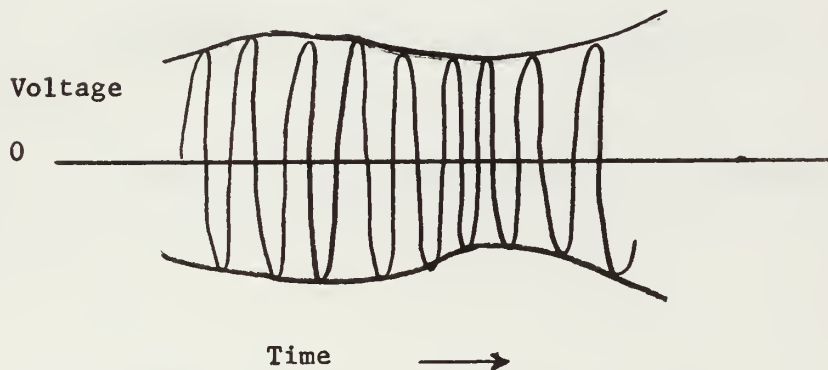


Figure 3-1 Synchro Voltage vs. Time

Because the voltage out of any phase can be expressed as a sine function of the bearing, bearing rate voltage will likewise be a sine function of the

bearing of the target.

Electrical differentiation of rectified sonar synchro bearing voltage is precluded as a feasible method of obtaining bearing rate because of the voltage ripple and the fact that bearing rate voltage is a function of both the bearing and the actual bearing rate. Differentiation always emphasizes noise.

Target bearing is proportional to the maximum (or RMS) amplitude of the carrier signal. If this synchro signal were to be applied at terminals "A" of a half-wave rectifier and holding circuit such as shown in Figure 3-2, then a voltage output similar to that in Figure 3-3 would result at terminal "B".

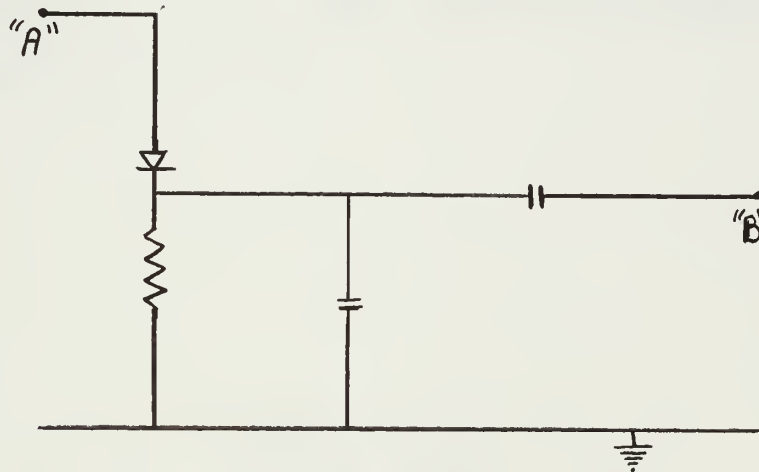


Figure 3-2 Half-wave Rectifier and Holding Circuit

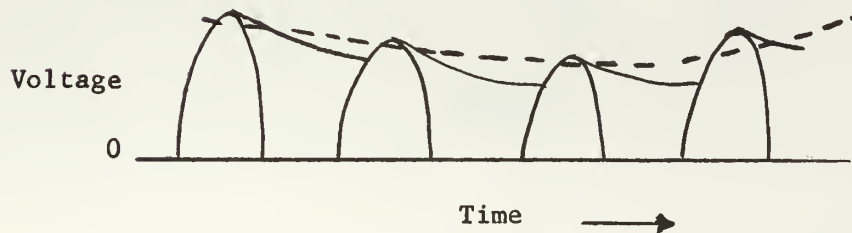


Figure 3-3 Output of Half-wave Rectifier and Holding Circuit vs. Time

This wave would then be sent through another stage of amplification in order to isolate the differentiat on circuit.

In Figure 3-3 the ripple has been emphasized. Ripple factor (r) can be expressed as:

$$r = \frac{\text{rms value of a-c components of wave}}{\text{average or d-c value of wave}}$$

If rectification were achieved such that the ripple factor were only 1% for a target with a constant bearing then there would be 400 very appreciable positive and 400 negative voltage outputs from the differentiator each second for a 400 cycle carrier. Possibly these oscillations might be averaged out by the meter used to display the bearing rate.

Amplitude of typical voltage outputs from the three phases of a synchro vs. bearing are shown below:

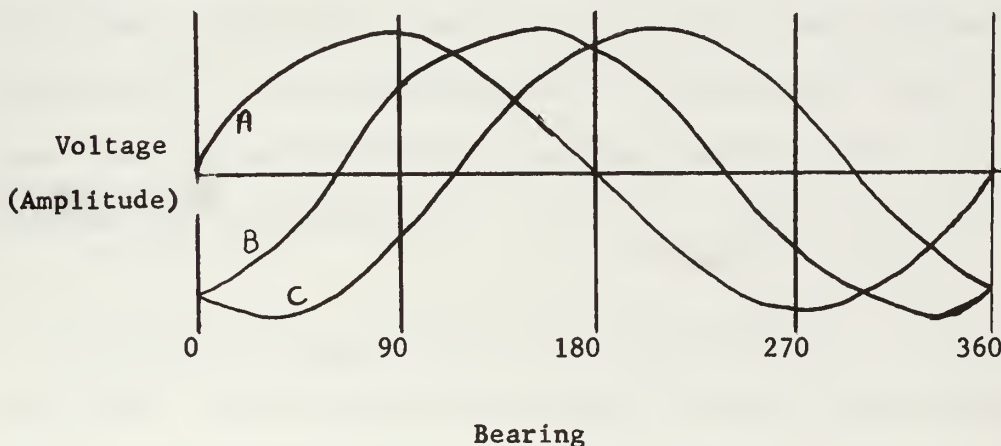


Figure 3-4 Synchro Voltages vs. Bearing

3.2 Position Servo Loop Operation

The next three devices which can possibly be used, utilize a position following servo loop. Operation of this loop is explained below.

Target bearing as transmitted by the sonar set is received by the synchro receiver. This receiver converts the electrical bearing to a mechanical rotational one; that is, output shaft rotation. Directly coupled to this shaft is a synchro transmitter which re-converts the shaft rotation into a three phase electrical signal which passes through a three pole relay prior to entering the the synchro control transformer. The reason for use of the synchro receiver and then the synchro transmitter is to insure that the bearing rate device is completely electrically isolated from the bearing transmission system on board the submarine. The relay is located between the synchro transmitter and control transformer in order that the device will not be "driven" while the sonar operator is searching for a target, shifting targets, or rapidly slewing for any reason. This relay closes the circuit to the control transformer upon energizing the 115 V 60 cycle light which is used to indicate that a target is being continuously and automatically tracked. The control transformer provides an error voltage (E) which is proportional to the difference between the electrical signal representing target bearing and the control transformer shaft position. This may be mathematically expressed as:

$$E = [k_s (\theta_R - \theta_C)] A$$

This error voltage is used, after amplification, to drive a two phase servo motor. The mathematical expression for the torque produced by an ideal two phase induction motor is:

$$T_M = \frac{\partial T_M}{\partial V} V + \frac{\partial T_M}{\partial \dot{\theta}_M} \dot{\theta}_M$$

Both $\frac{\partial T_M}{\partial V}$ and $\frac{\partial T_M}{\partial \dot{\Theta}_M}$ are virtually constants for most servo motors.

The torque produced by the motor is used to accelerate and drive the gear train which produces the follow-up rotation of the control transformer shaft and also turns the tachometer. An expression for this is:

$$T_M = T_{LOAD}$$

and

$$T_M = J \ddot{\Theta}_M + f \dot{\Theta}_M$$

The individual moments of inertia of each component such as shafts, gears, and rotors can be calculated mathematically to a very close degree and then be referred back to the motor. The ratio of friction to inertia can be rapidly determined by experiment.

3.3 Electronic Counter Device

Attached to the other shaft of the motor driven gearbox is a thin disc with perforations around its periphery. This is shown in Figure 3-6. Measurement of bearing rate is accomplished by using an electronic counter to measure the number of light pulses generated per unit time by the perforated wheel turning and interrupting a light which shines on a photo cell. Because the servo loop follows the target position, the wheel velocity will be proportional to target bearing rate as will the pulse count per unit time. In practice it would be necessary to use two photo cells and a phase sensitive network which could distinguish the pulses generated by rotation to the right from that to the left. It is also necessary to be able to take difference between the "right" pulses and the "left" pulses in order that a near constant bearing having slight oscillations which might be provided by the sonar set will not produce a very large bearing rate count.

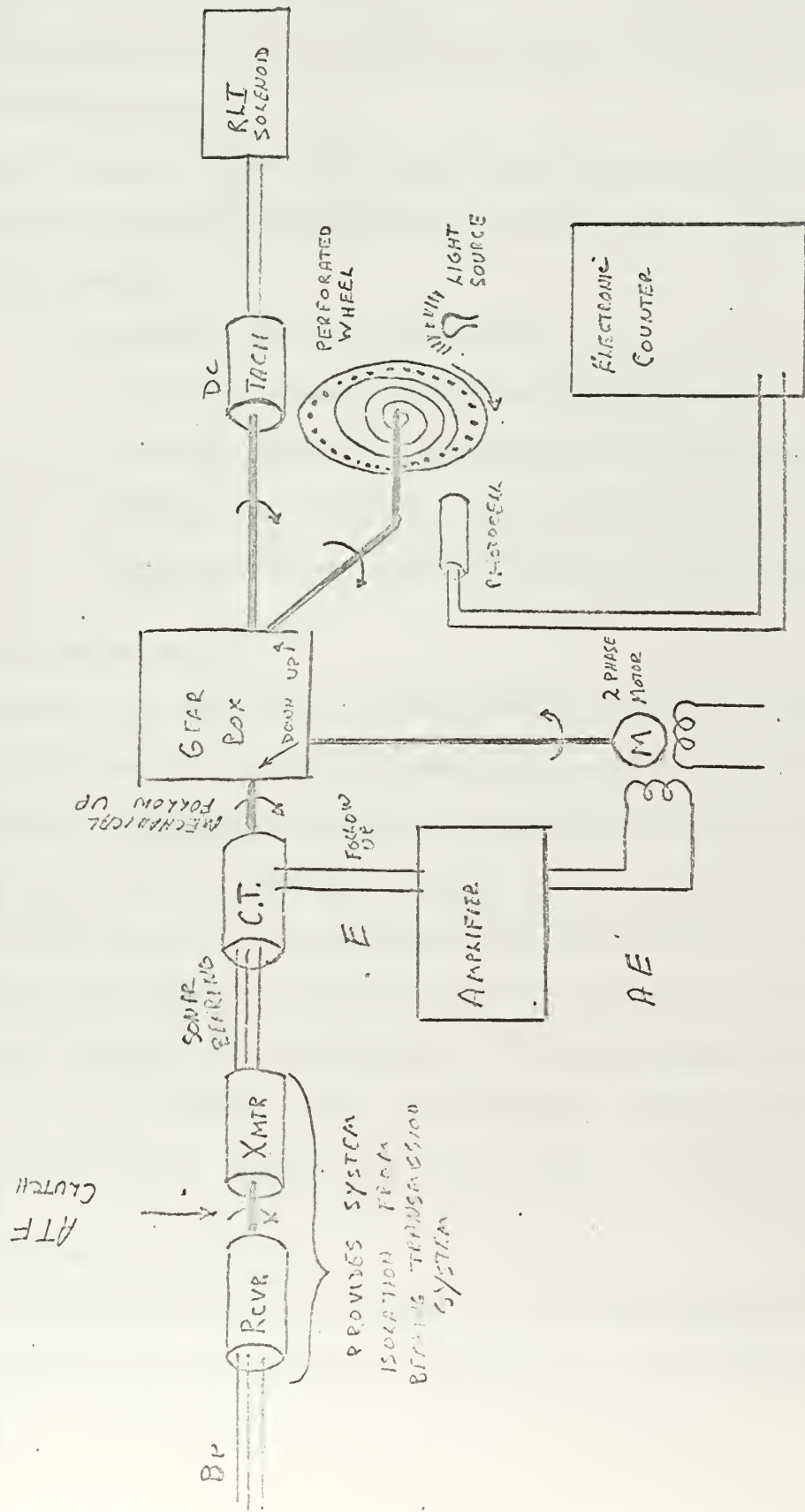


Figure 3-6

Worthy of note is the use of a tachometer to operate a right/left indicator. Also a spiral could be painted on the wheel and viewed through a slot so that as it rotated the short lines would appear to move inward or outward depending upon right or left bearing rates. This would be useful at very low bearing rates.

The primary advantage of this type device is the high probability of excellent accuracy in the determination of bearing rate. Disadvantages of this method include:

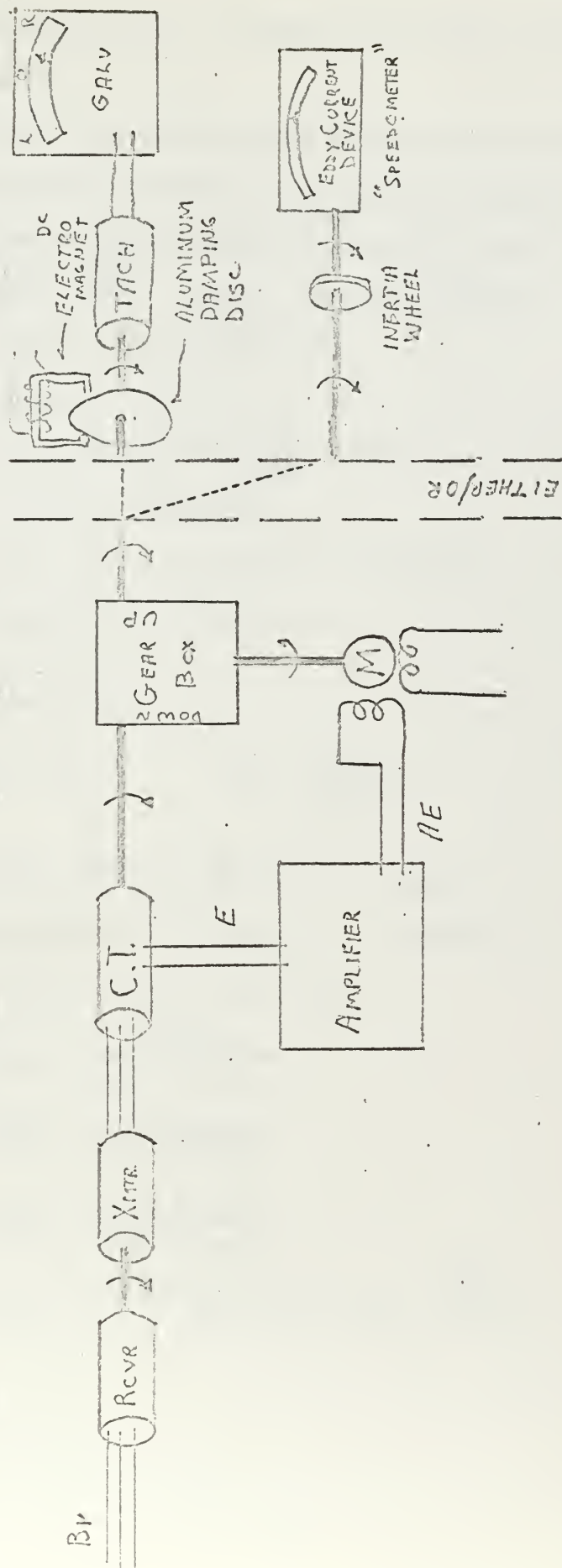
- 1) High cost of the counting device
- 2) Relatively complex, hard to maintain equipment
- 3) Circuitry required to distinguish between small right or left bearing rate pulses as the rate rapidly oscillates across zero degrees per minute would be involved and expensive.

3.4 Eddy Current Device

Instead of the perforated disc mentioned in the previous device, the second shaft from the gearbox is attached to an eddy current device as shown in figure 3-7. The eddy current device is nothing more than a speedometer similar to that on an automobile. Bearing rate is presented on this meter. The well known inaccuracy of speedometers and the difficulty of maintaining calibration are prominent disadvantages of this method of obtaining bearing rate. Also difficult is the achievement of different ranges such as 0 to 1 °/minute, 0 to 10 °/minute, and 0 to 100 °/minute. Physical shock could easily jar the device, causing loss of calibration of the instrument.

3.5 Galvanometer Device, Type A

The second shaft from the gearbox and associated gearing is not required because the error voltage is proportional to the bearing rate after



GALVANOMETER TYPE "B" and EDDY CURRENT TYPE DEVICES

Figure 3-7

transients have settled out. A diagram of the servo loop and equations is shown in Figure 3-8.

Manipulation of the block diagram of the servo loop and the equations in Laplace Transform form yields very interesting results. For convenience the equations in Laplace Transform form will now be listed and numbered.²

$$(I) \quad \Theta_r(s) = \frac{\dot{\bar{B}}_r}{s^2} \quad \text{because} \quad \Theta_r(t) = \left[\frac{\dot{\bar{B}}_r}{s^2} \right] [t]$$

$$(II) \quad E(s) = (\Theta_r(s) - \Theta_c(s))$$

$$(III) \quad V(s) = A E(s)$$

$$(IV) \quad T_M(s) = \frac{\partial T}{\partial V} V(s) + \frac{\partial T}{\partial \dot{\Theta}_M} s \Theta_M(s)$$

$$(V) \quad T_M(s) = T_{LOAD}(s)$$

$$(VI) \quad T_{LOAD}(s) = J s^2 \Theta_M(s) + f s \Theta_M(s)$$

$$(VII) \quad \Theta_c(s) = m \Theta_M(s)$$

For convenience let:

$$\frac{\partial T}{\partial V} = X \quad \text{and} \quad \frac{\partial T}{\partial \dot{\Theta}_M} = Y$$

Then:

$$T_M(s) = X V(s) + Y s \Theta_M(s) \quad \text{Form IV}$$

$$T_M(s) = [J s^2 + f s] \Theta_M(s) \quad \text{Form VI}$$

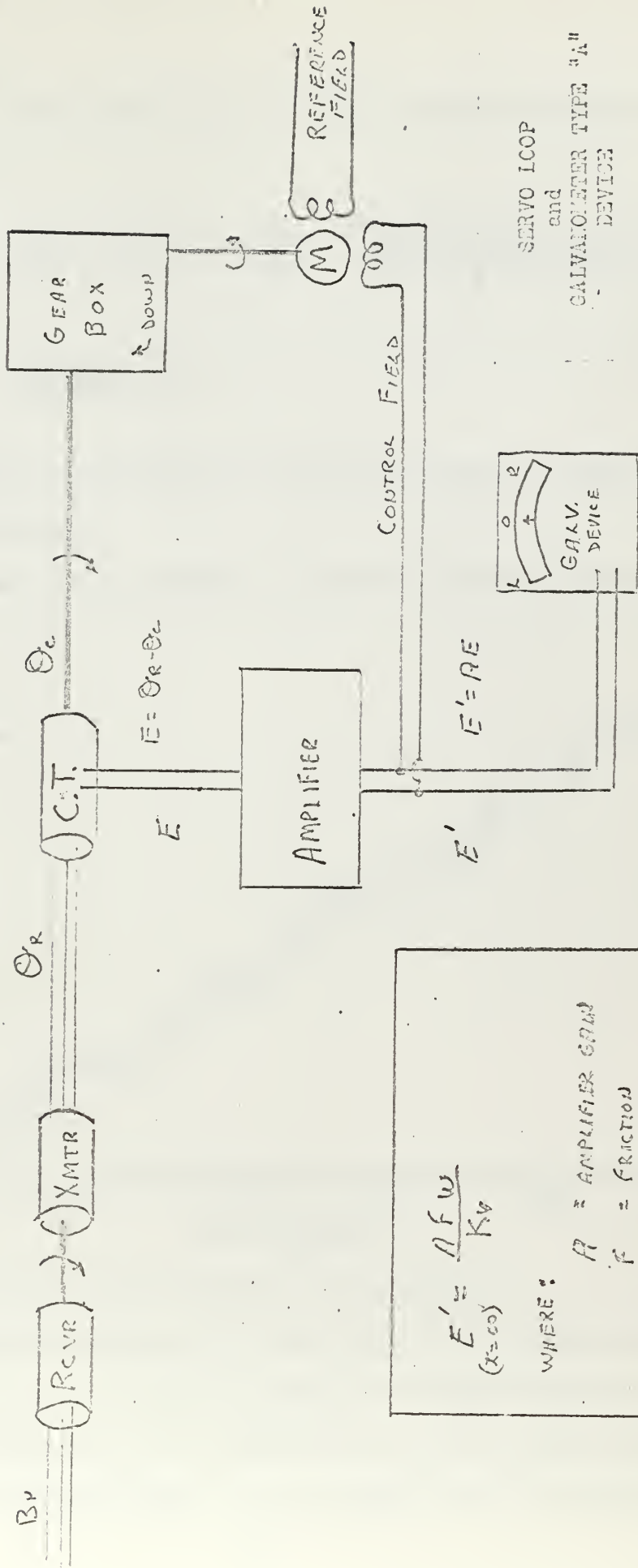
$$X V(s) = [J s^2 + (f - Y) s] \Theta_M(s)$$

$$\Theta_M(s) = \frac{X V(s)}{J s^2 + (f - Y) s}$$

$$\Theta_c(s) = \frac{m X V(s)}{J s^2 + (f - Y) s}$$

$$\Theta_c(s) = \frac{m X A E(s)}{J s^2 + (f - Y) s}$$

$$E(s) = \frac{J s^2 + (f - Y) s}{J s^2 + (f - Y) s + m X A} \left[\frac{\dot{\bar{B}}_r}{s^2} \right]$$



$$E' = \frac{A F \omega}{K_v}$$

($x = \cos$)

WHERE :

A = AMPLIFIER GAIN

F = FRICTION

K_v = SYSTEM VELOCITY COEFFICIENT

ω = ANGULAR VELOCITY
OR
BEARING RATE

Figure 3-0

Applying the final value theorem in order to obtain E steady state

$$E(t) = \lim_{t \rightarrow \infty} s [E(s)] = \lim_{s \rightarrow 0} s \left[\frac{Js^2 + (F-Y)s}{Js^2 + (F-Y)s + mXA} \right] \left[\frac{\dot{B}_r}{s^2} \right]$$

$$\lim_{t \rightarrow \infty} E(t) = \left[\frac{(F-Y)}{mXA} \right] \dot{B}_r$$

\dot{B}_r is therefore proportional to the error voltage, E, because F, Y, N, X, and A are constants.

Figure 3-9 shows the appearance of a typical continuous sonar bearing vs. time plot.

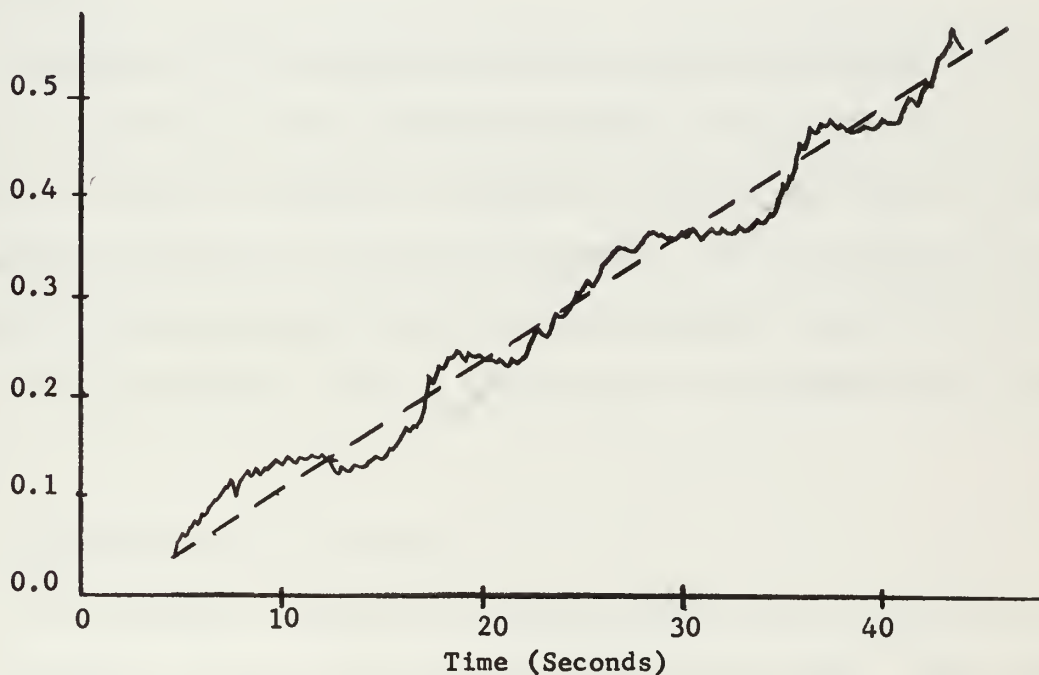


Figure 3-9 Sonar Bearing vs. Time (Typical)

The dashes show a constant slope line which would indicate a bearing rate of approximately 0.8 degrees per minute. The solid line shows the type of bearing response which can be expected from a passive sonar utilizing an automatic target following feature. This undashed curve can closely be

approximated by the constant sloped line with superposition of sine waves having an approximate period of 10 seconds plus some considerably higher frequency noise.¹ Because of the small amplitude as well as the noted frequency, the instantaneous derivative of synchro bearing as obtained by measuring the error voltage, E, would also be subject to significant error. (This also will be the case if electrical differentiation is attempted.)

3.6 Galvanometer Device, Type B

Basically the Galvanometer Device, Type B is very similar to the device just discussed. Rather than use the error voltage as a derivative indicator an additional gear train is attached to the motor and used to drive an A.C. tachometer. In general, tachometer output voltage proportional to its speed of rotation.

Smoothing of the oscillations and noise will be accomplished by utilization of the inertia of the rotating components. By using natural friction as well as negative feedback of tachometer voltage a very highly overdamped sluggishly responding system can be obtained. This can conceivably be adjusted to effectively ignore the undesired components and provide an output from the tachometer which is proportional to the dashed line of Figure 3-9.

3.7 Gyroscopic Precession Device

It is possible to construct a gyroscope which can be caused to process at an angular rate equal to the bearing rate of the target. This would require nothing but a rate gyro, one which is constrained to only one degree of freedom.

¹Based on Author's personal observation.

The rate gyro utilizes the precession phenomenon in which an angular velocity input produces an output torque. The differential equation for the torque $H\ddot{\theta}$ induced by precession must maintain the angle θ , accelerate the gimbal assembly about the torque axis, and overcome the axis damping moment is expressed by:

$$H\ddot{\theta} = J \frac{d^2\theta}{dt^2} + B \frac{d\theta}{dt} + K\theta$$

and

$$\dot{\phi} = \omega$$

where:

- j moment of inertia (gm-cm^2)
- K spring constant (dyne-cm/radian)
- H wheel angular momentum about spin axis (dyne-cm-second/radian)
- B viscous friction (dyne-cm-second/radian)
- ω input velocity or bearing rate (radian/second)
- θ angular displacement of H from torque axis (radians)

Figure 3-10 shows a diagram of a rate gyro.

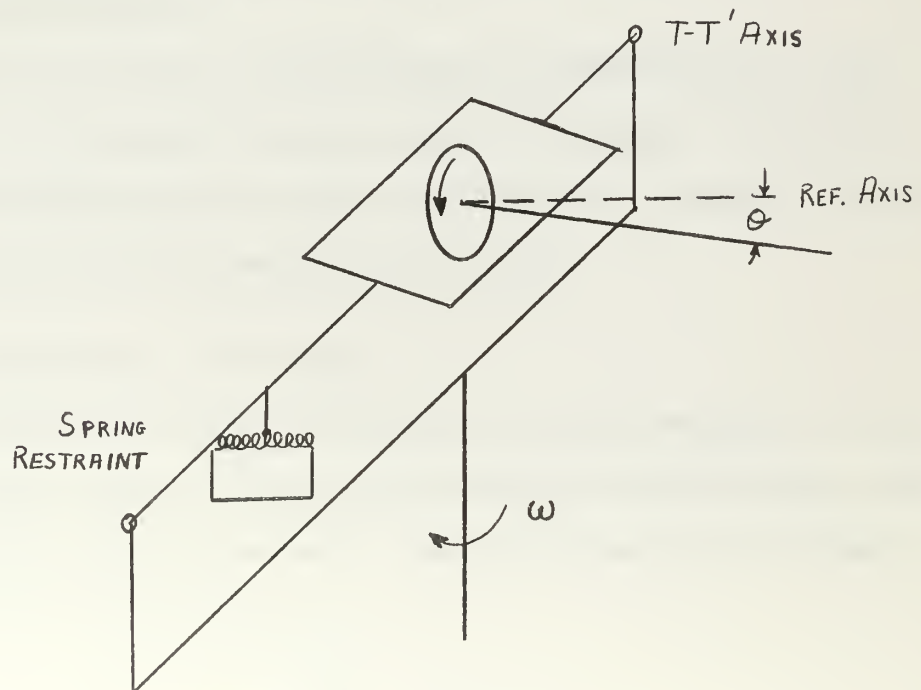


Figure 3-10 Rate Gyro

Taking the Laplace Transform of the differential equation for the gyro yields:

$$\frac{\Theta(s)}{\dot{\phi}(s)} = \frac{H}{Js^2 + Bs + K}$$

Investigating the response to a step velocity input of amplitude A gives:

$$\Theta(s) = \left[\frac{(\frac{H}{K})(\frac{A}{s})}{s^2 J/K + s B/K + 1} \right] \dot{\phi}(s)$$

The steady state response is found from:

$$\Theta(t) = \lim_{t \rightarrow \infty} s \left[\frac{(\frac{H}{K})(\frac{A}{s})}{s^2 J/K + s B/K + 1} \right] \dot{\phi}(s)$$

and equals,

$$\Theta(t) = \frac{HA}{K} \dot{\phi}$$

This shows that if the input to a rate gyro is $\dot{\phi}$ the output angle Θ is directly proportional to $\dot{\phi}$. The output angle can be easily converted to an electrical signal and amplified if desired.

The primary difficulties tending to exclude choice of this system are:

- 1) Gyro devices are complex, expensive, and generally require sophisticated power supplies.
- 2) Some constraint is required upon the maximum angle of precession. This is true because the gyro cannot be physically permitted to have an infinite rotation about its axis of precession. Therefore resetting to a neutral position will be periodically required.

3.8 Choice of Type Device to be Tested

The entire previous section was devoted to a brief inspection of some 8 different possible means of cheaply and accurately obtaining bearing rate from continuous sonar synchro bearings. Completely ruled out by probable

excessive expense are:

- 1) a least squares fit by means of a sampled
bearings to a small special purpose digital computer prior
to differentiation

and

- 2) optimum filtering of the bearing signal by digital means
prior to differentiation.

If the previous discussion and the preceeding comments are valid there is therefore only one method which appears to merit additional attention in order to produce a device which might fulfill the requirements set forth in Section 2-b. A device similar to the one identified as "Galvanometer Device, Type B" is the obvious choice and an attempt was made to produce an initial prototype by this system.

SECTION 4

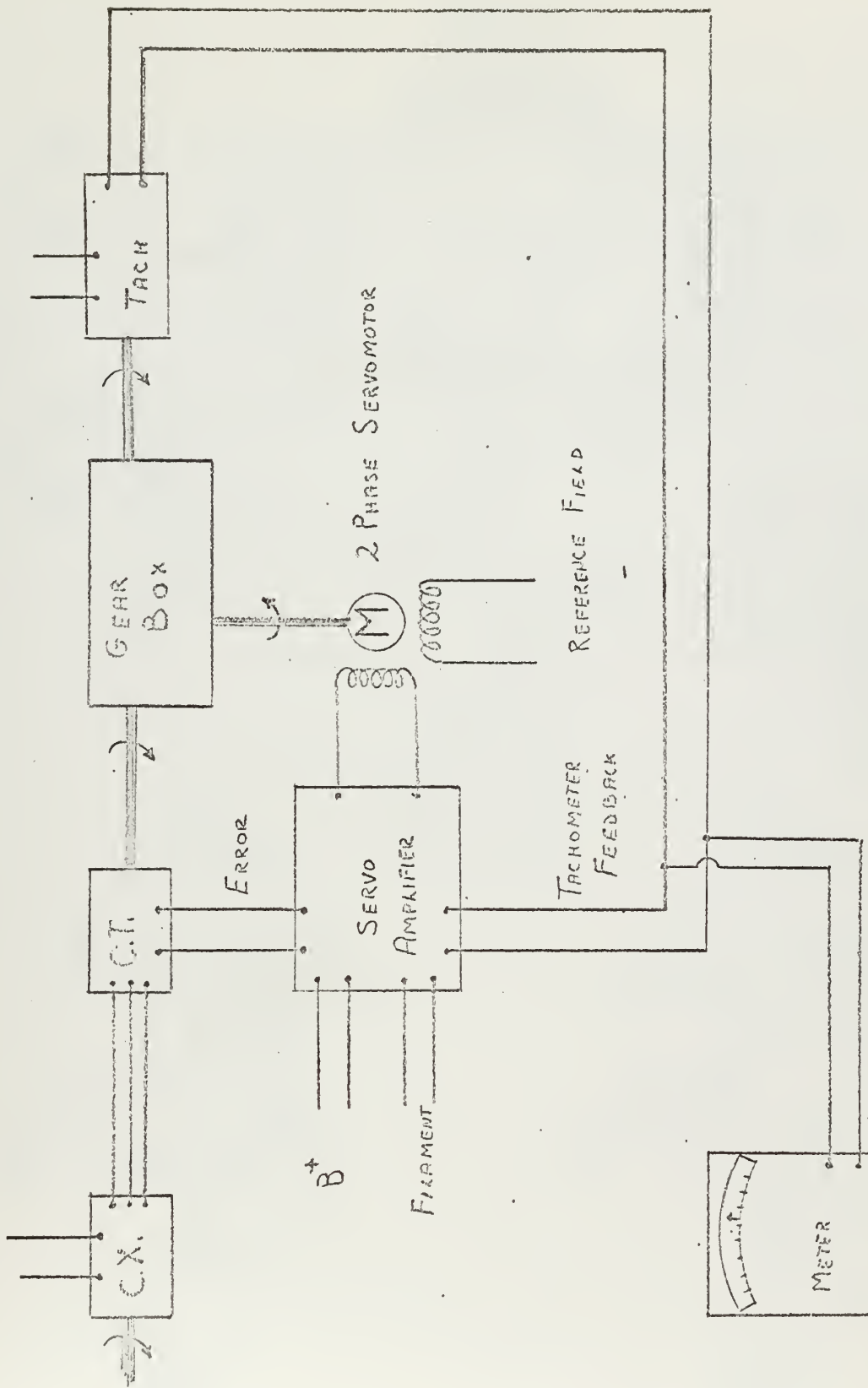
4. Development of Initial Prototype Bearing Rate Device

4.1 Description of Initial Prototype Device

It was desired to insure the validity of the reasoning used in choosing the type bearing rate device to be developed. In order to do this without excessive expenditure of government funds, the Initial Prototype Device was fabricated and tested using items which were readily available at the U. S. Naval Postgraduate School. This was done with full realization that the components which were to be utilized were often far from ideal.

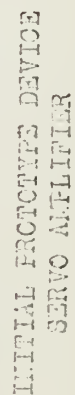
Figure 4-1 is a diagram of the initial prototype device. The components used were:

- a) Servomotor, Kearfott R112, 120V, 2 phase 400 cycle
- b) Tachometer Generator, Kollsman 04300, Reference 55V, 400 cycle
- c) Synchro Transmitter, Bendix Autosyn 26V, 400 cycle
- d) Control Transformer, Bendix Autosyn, 26V, 400 cycle
- e) Gear Box - gear ratio of approximately 50:1 between motor control transformer shaft
- f) Transformer 120 volt 400 cycle to 26 and 55 volt for synchro and tachometer supply voltages respectively.
- g) A Servo Amplifier which consisted of two identical preamplifier channels with provisions for phase adjustment of each channel. The outputs of the pre-amplifier stages were added and then sent to a twin triode amplifier and phase inverter prior to a push-pull output stage. A circuit diagram of the amplifier is shown in Figure 4-2. Symbols used on the diagram are:



INITIAL PROTOTYPE DEVICE
SCHEMATIC DIAGRAM

Figure 4-1



22

- 1) G_e error preamplifier, gain control
- 2) G_t tachometer preamplifier gain control
- 3) P_e error channel phase adjust
- 4) P_t tachometer channel phase adjust
- 5) G amplifier gain control
- 6) T.P. circuit test points for phase adjustment

In order to operate, evaluate constants, determine transfer functions and evaluate the response of this prototype, the following equipments were utilized:

- a) A Dynamic Analyzer, Industrial Control Company, Type 100A
- b) Oscilloscope, Hewlett Packard, Model 120B
- c) Oscilloscope, Dumont, Type 304H
- d) Regulated Power Supply, Universal Electronics, Model 520A, 0-300V DC (used for B+ on amplifier)
- e) Transistorized Power Supply, Power Designs Inc., Model 3240 (used for 6.3V DC to amplifier filaments in order to reduce filament noise.)
- f) Camera, Polaroid, Model 196A.

4.2 Obtaining Constants from Initial Prototype Device

a. Moment of Inertia, J.

The various moments of inertia for the components of the gear train from the weight and diameter of each element. Each of the gears and the shafts closely approximated a right circular cylinder the individual moment of inertia about its longitudinal axis could be calculated.

$$J \equiv \int_{r_1}^{r_2} r^2 dm$$

(for any body)

where: J is the moment of inertia

dm an element of body mass

r the distance of the mass element from the axis

For the case of the right circular cylinder it can be shown that:

$$J = \frac{1}{2} m r^2$$

where: r is the outer radius of the cylinder

Figure 4-3 illustrates the gear train showing component locations.

Table 4-1 lists the moments of inertia of each gear and shaft. Table 4-2 shows the nominal moment of inertia for the motor, tachometer, and control transformer as given by their respective manufacturers. Table 4-3 gives the various gear ratio data as computed by use of the CDC Model 1604 Digital Computer in "Program Gear 2" as shown in Appendix A.

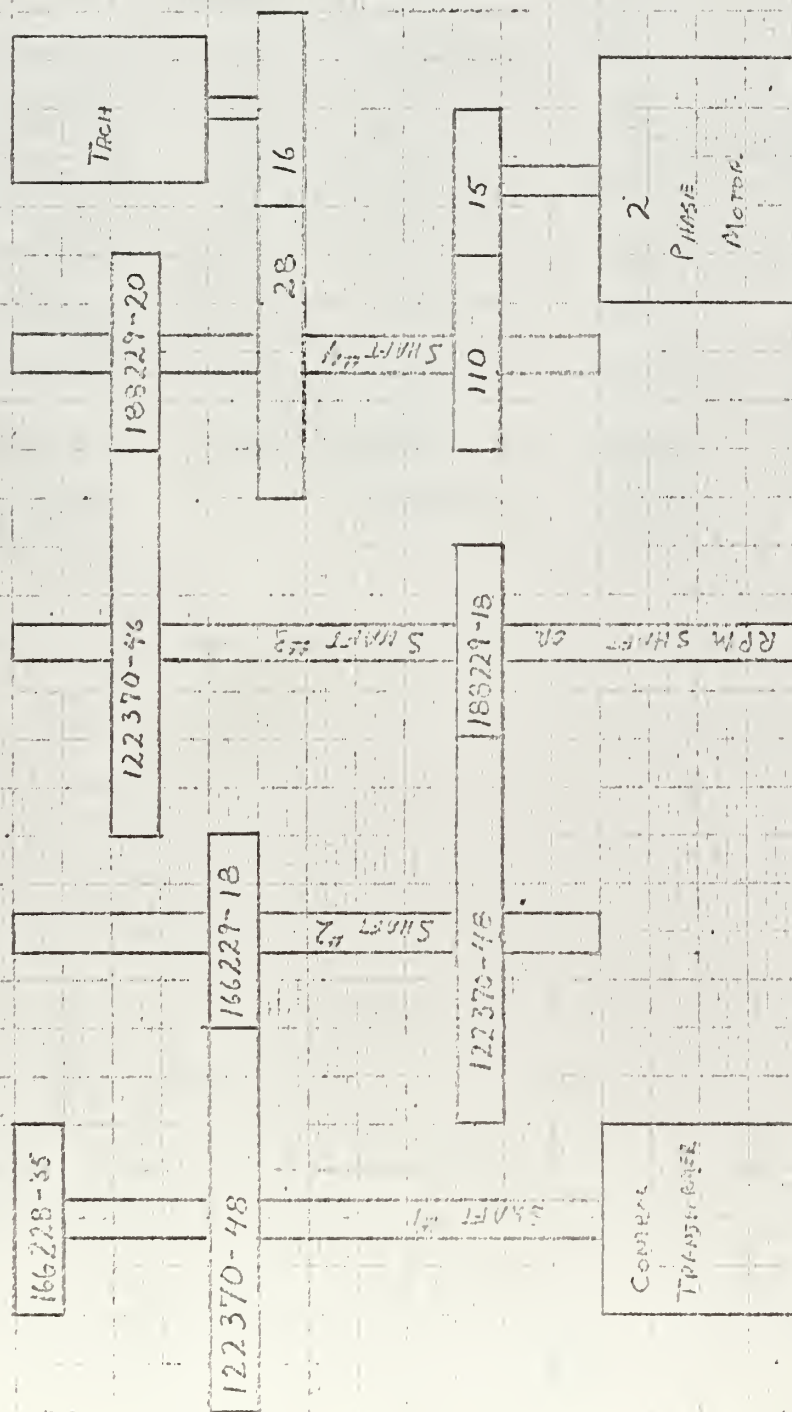
It can be easily shown from power and torque considerations that moments of inertia on one side of gearing may be "translated" to the other side of the gearing if multiplied by the square of the gear ratio.²

"Program Totiner" in Appendix A gives the computation of the total moment of inertia of the geared system as seen at the motor shaft. This resulted in a value of J at the motor shaft of 5.755 gram-centimeters square.

b. Determination of Friction Factor, F

The ratio of the friction factor, F , to that of the inertia, J , was determined by means of a retardation test as outlined in part 1 of Appendix B. Multiplication of this F/J ratio was accomplished and is also shown in "Program Totiner" of Appendix A. The value of F as determined was 15.567 gram centimeters per second.

²Thaler, G. T. and Brown, R. G. Analysis and Design of Feedback Control Systems, pp. 37-40, McGraw-Hill Book Co., Inc., New York, 1960.



Note: The last group of numbers shown on each gear indicate the number of teeth.

INITIAL PROTOTYPE DEVICE GEAR TRAIN AND COMPONENTS

Figure 4-3

TABLE 4-1 INITIAL PROTOTYPE GEAR AND SHAFT MOMENTS OF INERTIA

GEAR DESIGNATOR	NUMBER OF TEETH	WEIGHT (GRAMS)	DIAMETER (INCHES)	DIAMETER (CM)	J_2 GM-CM ²
166228-35	35	28.76	1.47	3.75	50.555
122370-48	48	25.50	2.031	5.16	84.869
166229-18	18	13.82	.844	2.14	7.911
- - - -	110	13.85	1.156	2.94	14.964
122370-46	46	24.05	1.969	5.00	75.156
188229-20	20	16.21	.938	2.38	11.477
166228-28	28	20.20	1.1975	3.017	22.983
166229-16	16	11.50	.750	1.905	5.217
Shaft #1	--	47.50	.3125	.794	3.743
Shaft #2	--	28.10	.3125	.794	2.214
Shaft #3	--	49.87	.3125	.794	3.930
Shaft #4	--	19.80	.3125	.794	1.560

TABLE 4-2 MOTOR, TACHOMETER, AND CONTROL TRANSFORMER DATA FOR INITIAL PROTOTYPE

MOTOR -

Kearfott
Size 18
Type R112-2D 400 cycle 115 volt
Serial 637
 $J=4.0 \text{ gm-cm}^2$

TACHOMETER

Kollsman
Type 863-043000
Serial 12488
 $J=2.60 \text{ gm-cm}^2$

CONTROL TRANSFORMER

Bendix Autosyn
Serial 14117
 $J= 1.5 \text{ gm-cm}^2$

TABLE 4-3 GEAR RATIO DATA

RATIO TO MOTOR

Shaft Ratio

A	.136363636
B	.059388538
C	.022233202
D	.008337451
E	.238636364

RATIO TO MOTOR SQUARED

Shaft Ratio Squared

A	.018595401
B	.003515131
C	.000494315
D	.000069513
E	.056947314

OVERALL RATIO FROM FAR
SIDE OF SHAFT TO MOTOR
SIDE OF SHAFT

Shaft Ratio

A	.136363636
B	.434782609
C	.375000000
D	.375000000
E	1.75000000

Note: Ratios shown are going away from motor.

c. Summary of Constants, Coefficients, and Parameters Obtained

These are summarized in Table 4-4 .

d. Block Diagrams for Initial Prototype

A block diagram of this system is shown in Figure 4-4. Figure 4-5 shows the system block diagram in the form required for use in "Program Analog." This program is a digital computer simulation of an analog computer which was written by LT Joseph D. Fenick, USN.

Simulation of the system was accomplished by use of an E.A.I. TR20 analog computer. The block diagram of Figure 4-4 was manipulated into the form of Figure 4-6 for analog computer simulation. Complete block reduction of the system produces the following transfer function:

$$\frac{V_T}{B_r} = \frac{2.195 K_e}{s(s^2 + (57.414 + 4.32 K_T)s + 1.117 K_e)}$$

TABLE 4-4 CONSTANTS AND PARAMETERS FOR INITIAL PROTOTYPE DEVICE

Control Transformer Sensitivity	.508 volts/degree
---------------------------------------	-------------------

$\frac{\partial T_M}{\partial V}$	1470 $\frac{\text{dyne cm.}}{\text{volt}}$
-----------------------------------	--

$\frac{\partial T_M}{\partial \dot{\theta}_M}$	305 $\frac{\text{dyne cm.}}{\frac{\text{radian}}{\text{second}}}$
--	---

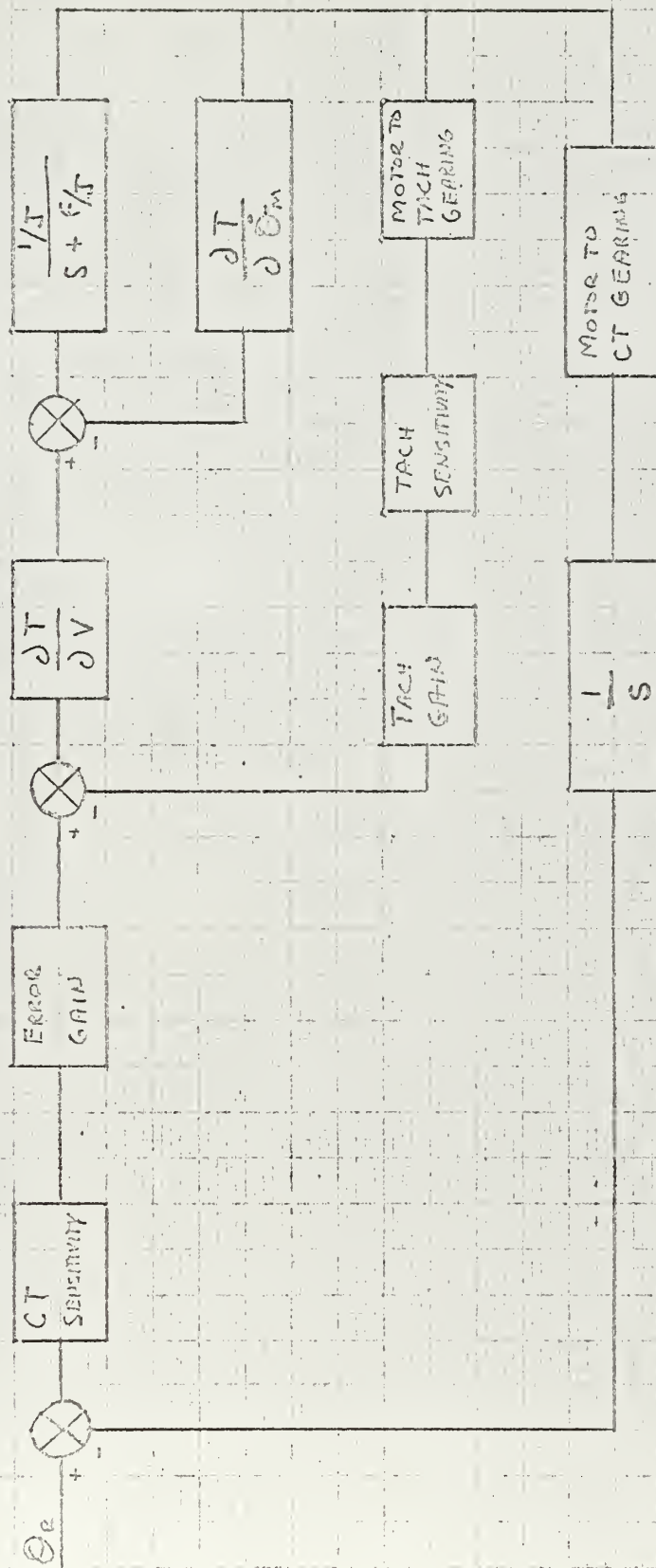
Tachometer Sensitivity	-.685 $\frac{\text{volts}}{\frac{\text{radian}}{\text{second}}}$
---------------------------	--

Motor to Tachometer Gear Ratio	.238636364
--------------------------------------	------------

Motor to CT Gear Ratio	.008337451
---------------------------	------------

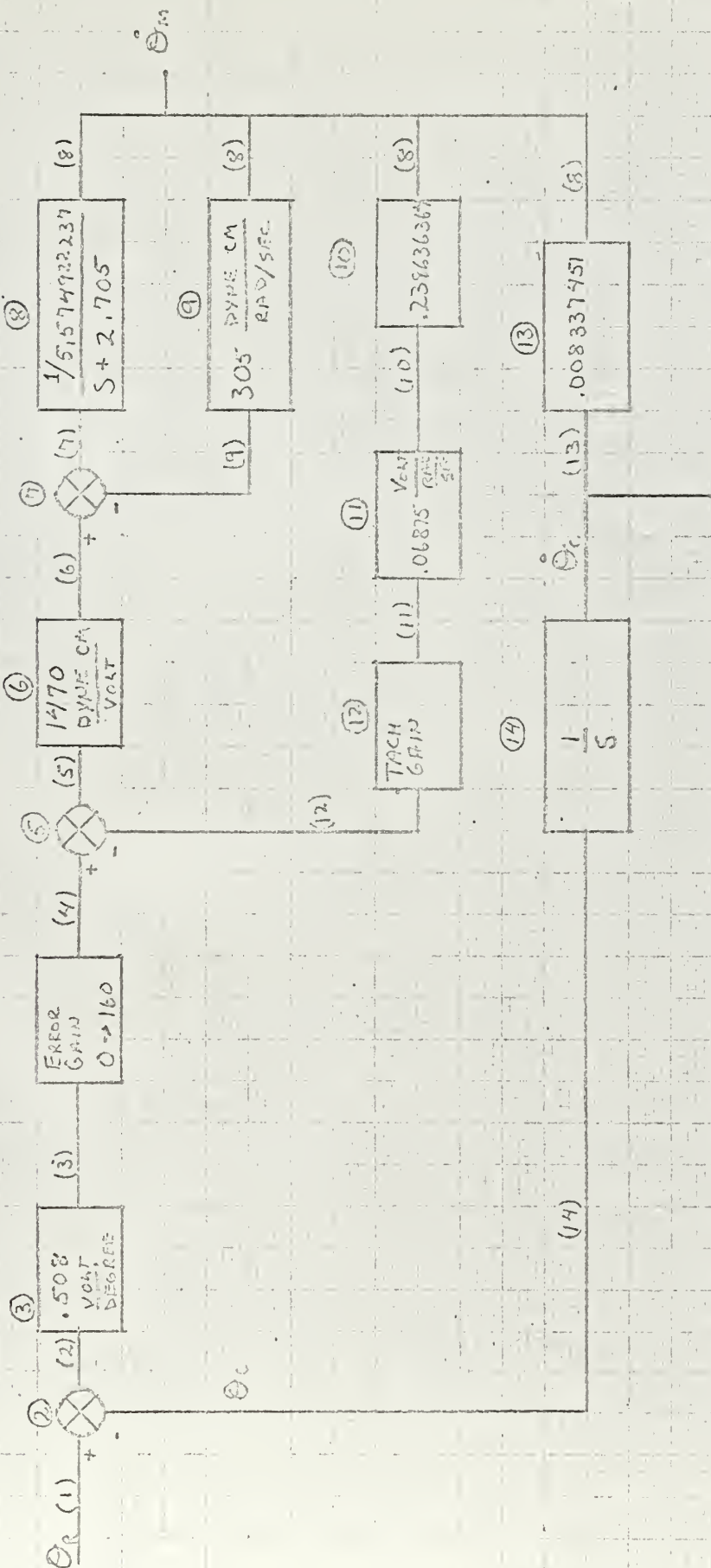
f/J Ratio	2.705
-----------	-------

J	5.5749 gm-cm ²
---	---------------------------



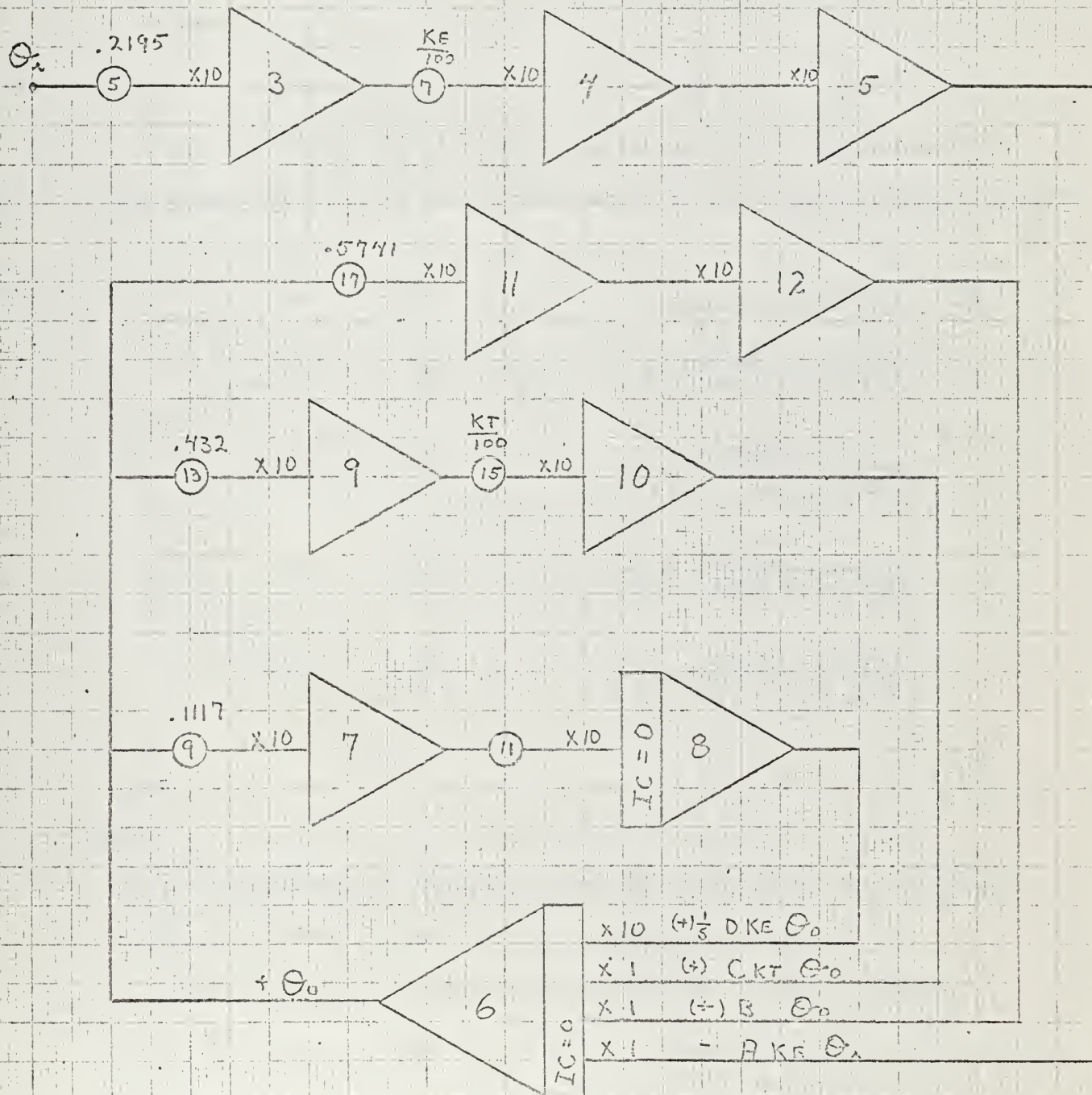
INITIAL PROTOTYPE DEVICE BLOCK DIAGRAM

Figure 4-4



INITIAL PROTOTYPE DEVICE PROGRAM ANALOG BLOCK DIAGRAM

Figure 4-5



INITIAL PROTOTYPE DEVICE ANALOG COMPUTER SIMULATION

Figure 4-6

The constants A, B, C, D have been used for simplicity and were:

$$A = 2.195$$

$$B = 57.414$$

$$C = 4.32$$

$$D = 1.117$$

With settings of both tachometer and error channel potentiometers lying between 10 and 100, the extreme ranges of the transfer function were:

KE	KT	Transfer Function For $\frac{V_T}{\dot{\theta}_r}$
10	10	$\frac{21.95}{s(s^2 + 100.6s + 11.17)}$
100	10	$\frac{219.5}{s(s^2 + 100.6s + 111.7)}$
10	100	$\frac{21.95}{s(s^2 + 489.4s + 11.17)}$
100	100	$\frac{219.5}{s(s^2 + 489.4s + 111.7)}$

where:

V_T represents the bearing rate voltage produced by the tachometer

$\dot{\theta}_r$ represents the bearing rate in degrees per minute

Digital computer factoring of these transfer functions yielded:

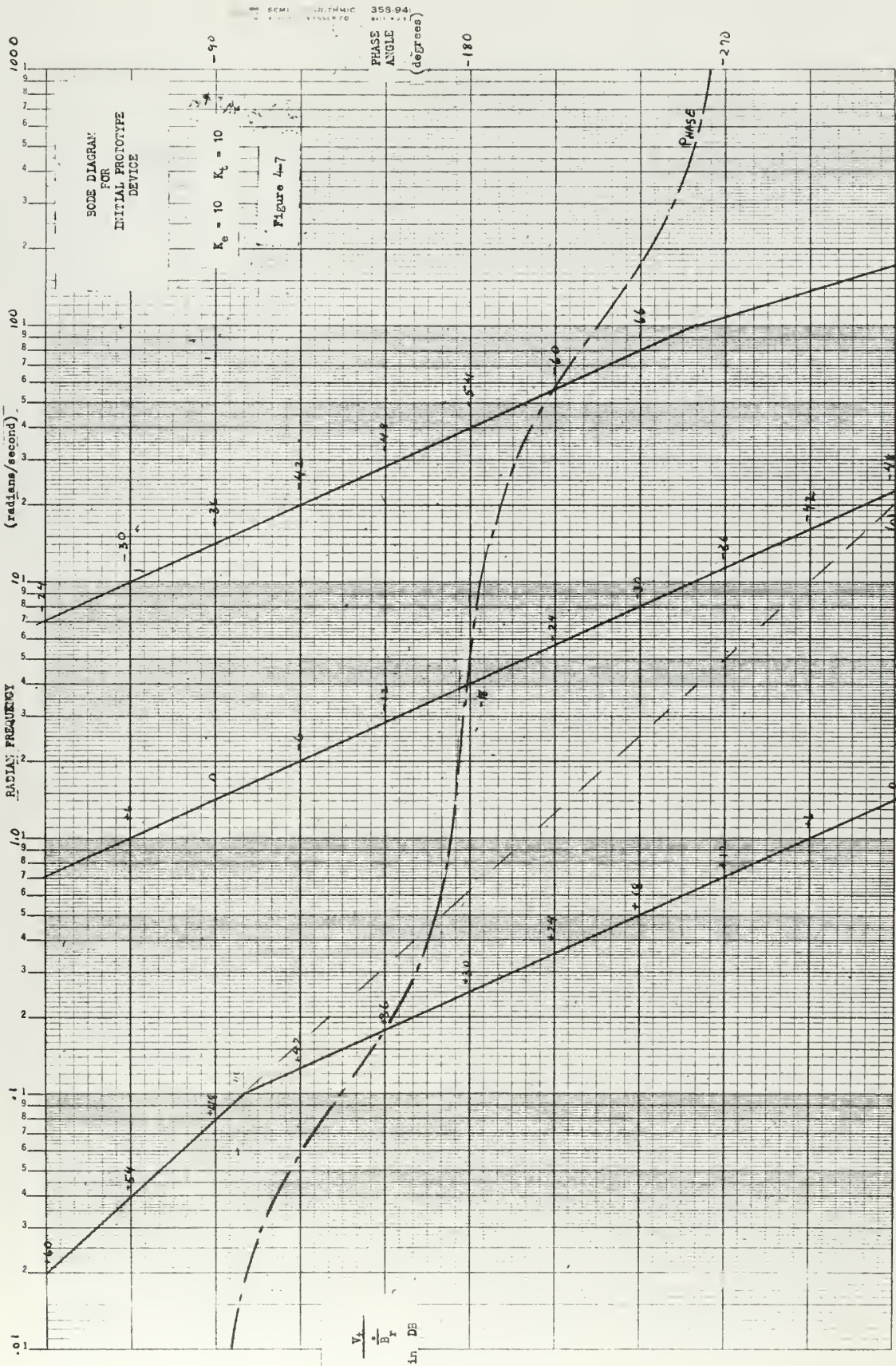
KE	KT	Factored Transfer Function	Bode Diagram
10	10	$\frac{21.95}{s(s + 1.111)(s + 100.47)}$	4-7
100	10	$\frac{219.5}{s(s + 1.1229)(s + 99.47)}$	4-8

KE	KT	Factored Transfer Function	Bode Diagram Figure #
10	100	$\frac{21.95}{s(s+.022825)(s+489.38)}$	4-9
100	100	$\frac{219.5}{s(s+.22835)(s+489.17)}$	4-10

The Bode diagrams give some feeling for the effect of varying KE and KT. The required upper limit of bearing rate was chosen 100°/minute. By using the 10° per revolution bearing transmission system this minimum upper limit of target bearing rate can be expressed as 1.0472 radius per second. To achieve adequate response it is then necessary to adjust KE and KT such that the zero DB point of the gain curve is located slightly to the right of 1.0472 radius per second. This insures adequate response as well as assisting in rejection of undesired noise having frequencies above the upper limit of bearing rate. In effect the entire servo loop is being used to take the derivitative of the output of a very low pass filter.

4.3 Bearing Rate Device Feasibility

The Initial Prototype Device was analyzed by means of both an analog and a digital computer. Because of the very high gain required in several cascaded operational amplifiers some difficulty was experienced with amplifier saturation. "Program Analog" on the CDC 1604 digital computer was used to check the validity of the analog computer results. Figure 4-11 shows the results of the use of the analog computer. This figure clearly indicates the feasibility of a bearing rate device using a position following servo loop driving an a.c. tachometer.



BODE DIAGRAM FOR INITIAL PROTOTYPE DEVICE

$K_0 = 100 \quad K_c = 10$

Figure 4-3

MAGNITUDE (dB) vs. FREQUENCY (rad/sec)

PHASE (deg) vs. FREQUENCY (rad/sec)

Annotations: 0.1, 1, 10, 100, 0, 10, 20, 30, 40, 50, 60, 70, 80, 90, 100, -90, -80, -70, -60, -50, -40, -30, -20, -10, 0, 10, 20, 30, 40, 50, 60, 70, 80, 90, 100

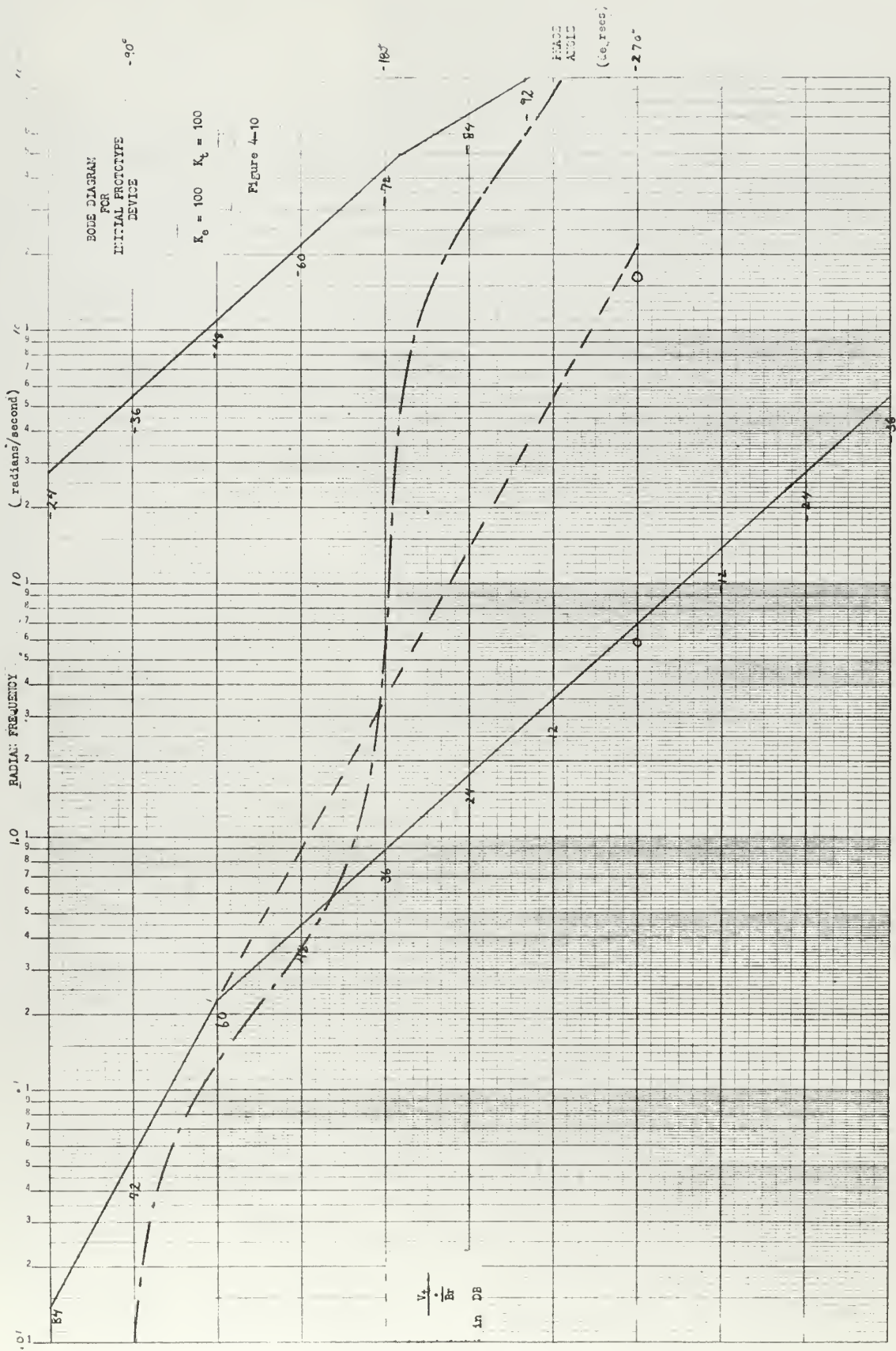
Figure 48.

[illegible]

PHASE

-270

$\frac{V}{B_r}$ in D3



STEADY STATE
TACHOMETER VOLTAGE
(volts)

BEARING RATE
(degree/minute)

LEFT

+20

+10

0.0

0

RIGHT

10

20

30

INITIAL PROTOTYPE DEVICE
STEADY STATE
TACHOMETER VOLTAGE
vs.
BEARING RATE

Figure 4-11

SECTION 5

5. Development of Final Prototype Device

In the preceeding section it was shown that a very low pass differentiating filter could be developed utilizing the electro-mechanical properties of a position following servo loop and tachometer. Incompatability of the bulky and expensive power supplies for the vacuum tube servo amplifier with the requirements for a small and inexpensive device precluded acceptance of the initial prototype device.

5.1 Final Prototype Servo Loop

It was anticipated that, in order to save money, the servo loop of the final prototype device would utilize several of the same components that had been used in the initial prototype such as the two phase motor, the a. c. tachometer, and the synchros. The primary changes were expected to be the substitution of a magnetic or transistorized sixteen watt (or greater), 400 cycle, servo amplifier having its own internal power supplies, an improved gear train, and an improved read out device.

The major components which were actually used in the Final Prototype were:

(a) Servo amplifier, 120 volt, 400 cycle, BUORD Drawing #1836748, Librascope Group, General Precision, Inc.

(b) Input network for the above servo amplifier, BUORD Drawing #2075721, Librascope Group, General Precision, Inc.

(c) Synchro transmitter (CX), 120 volt, 400 cycle, Type 15CX4, Ketay Corp.

(d) Synchro control transformer (CT), 120 volt, 400 cycle, Type 15CT4, Ketay Corp.

(e) Motor-generator, Mark 12-0, 120 volt, 400 cycle, Type 15TGSM4, Kearfott Division, General Precision, Inc.

(f) Audio amplifier, 120 volt, 60 cycle, Model 904 Trutone Electronics.

(g) Anti-backlash, split-type spring-loaded precision gears, Dynamic Gear Co., Inc.

(h) Compensated wattmeter, 0-10 watts, Type 1379, Simpson Electric Co.

Circuit diagrams for the servo amplifier, BUORD DRAWING #1836748, and its input network, BUORD DRAWING #2075721, are shown in Figures 5-1 and 5-2. Use of this amplifier and input network required a change from the motor and tachometer as were anticipated to a Mark 12 motor-generator. This was done in order that the motor and the tachometer be completely compatible with the transistorized amplifier and its internal power supplies. Use of 120 volt 400 cycle synchro was made so that the need for a synchro and tachometer supply transformer might be eliminated.

While the other components for the servo loop were being acquired the precision gear train from the motor to the control transformer was being built in the machine shop at the United States Naval Postgraduate School. This gear train was constructed of 96 pitch, 20 degree pressure angle split-type anti-backlash precision gears. This gear train is shown in Figure 5-3. One unfortunate result of the decision to use the Mark 12 motor-generator was that its no-load speed is only 4700 RPM as opposed to 9800 RPM for the Kearfott R112 motor. Use of this motor-generator and the gear train as designed lowered the maximum bearing rate obtainable to approximately 48 degrees per minute. In addition, replacement of the Kollsman

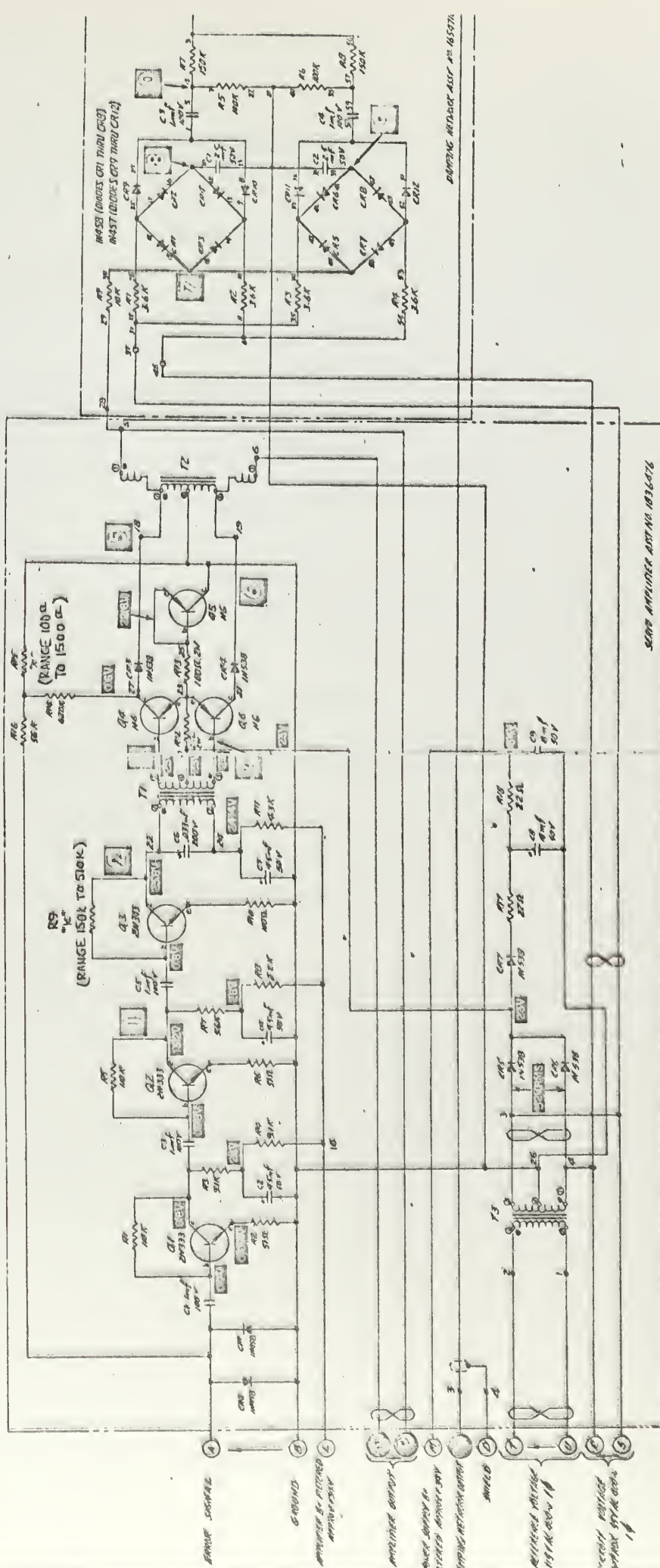


Figure 5-1

FINAL PROTOTYPE DEVICE
SERVO AMPLIFIER
CIRCUIT DIAGRAM

BUORD DRAWING #1836743

SYNCHRO AMPLIFIER INPUT NETWORK

BUCRD DRAWING #2075721

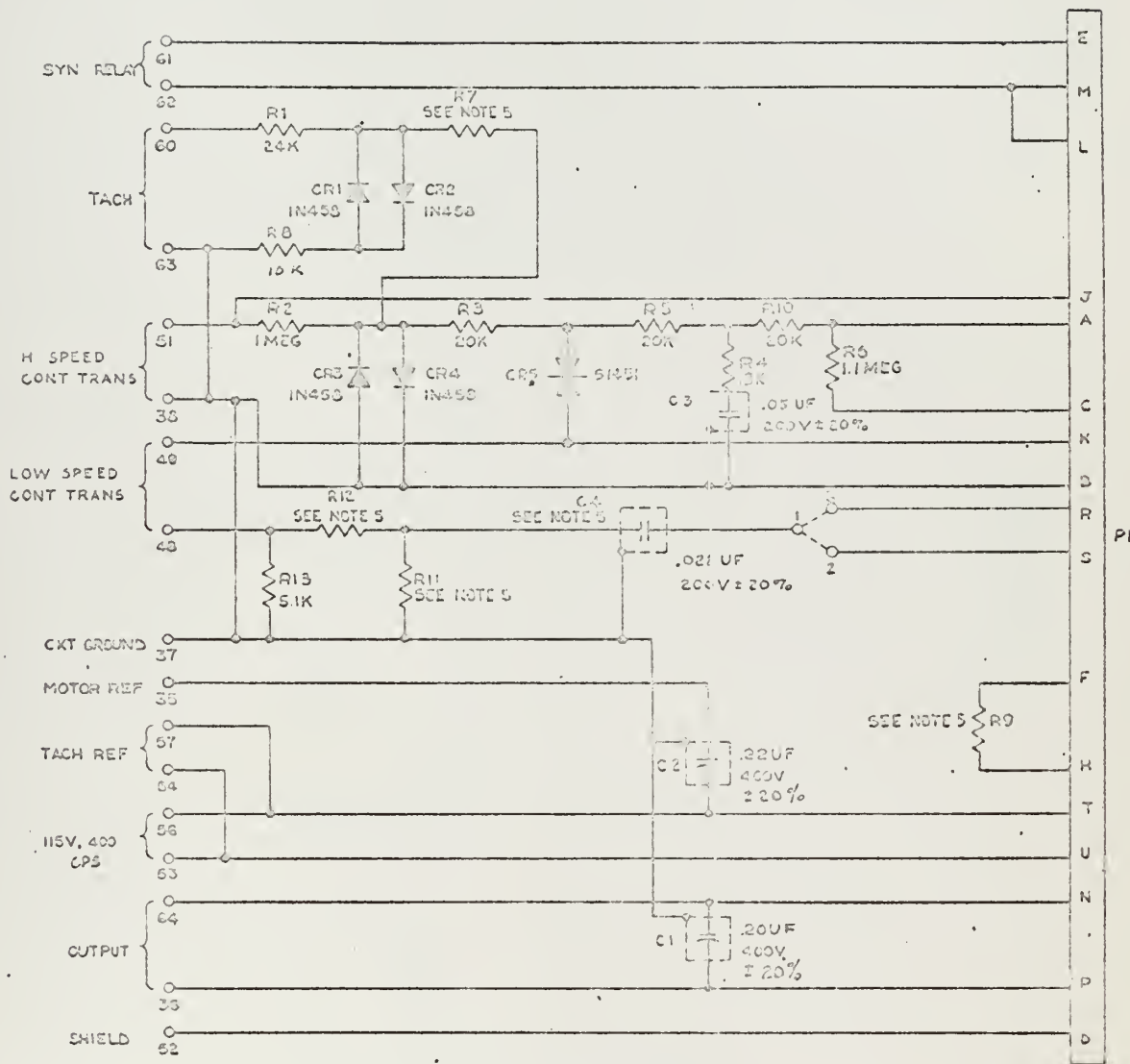
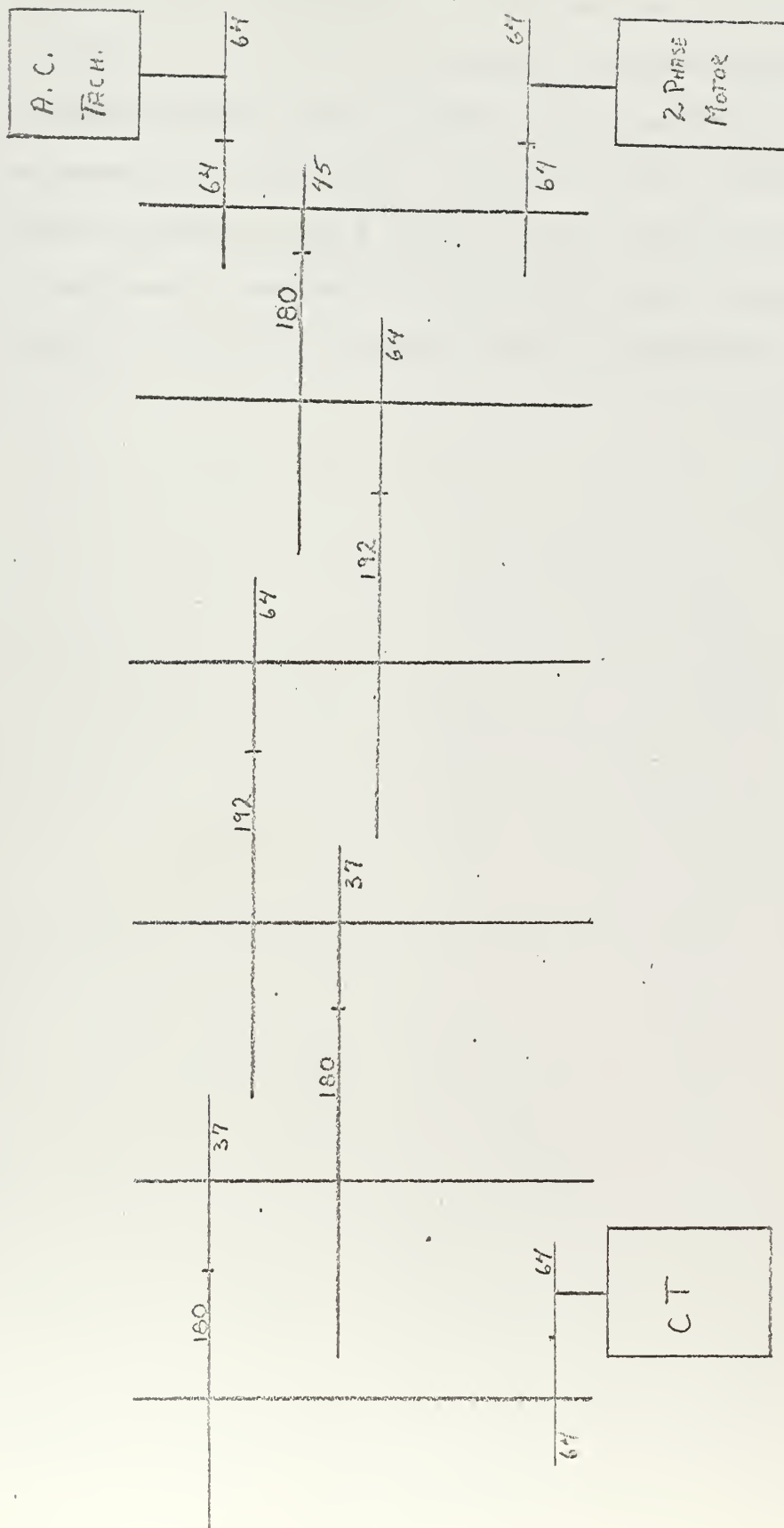


Figure 5-2



Note: The numbers by each gear represent the number of tooth on that gear.

FINAL PROTOTYPE GEAR TRAIN

Figure 5-3

tachometer by the Mark 12 motor-generator lowered the tachometer output voltage from 7.17 volts per 1000 RPM to only 3.1 volts per 1000 RPM.

A possible slight improvement in performance was to be expected by the elimination of any effects of backlash in the gearing between the motor and the tachometer because the Mark 12 motor-generator has the motor and tachometer on the same shaft. It was later found necessary to use a separate tachometer from a Mark 12-0 motor generator because a 1.0 to 1.5 volt peak to peak 400 cycle tachometer output was observed at zero velocity. The cause of this was traced to leakage flux from the motor.

5.2 Bearing Rate Meter

In sections 3 and 4 it was established that the voltage output from the tachometer was proportional to bearing rate. Until development of the final prototype was attempted it was not noted that no means existed by which an a.c. voltage indicating a right bearing rate could be distinguished from the a.c. voltage indicating a left bearing rate. By using a wattmeter with the current (or voltage) coil supplied by the tachometer output and the voltage (or current) coil from the tachometer or reference supply voltage, meter deflections to the right could be obtained for right bearing rates and to the left for left bearing rates.

In order to provide a small, easily read, accurate reading meter a Simpson 10 watt compensated wattmeter was purchased. One difficulty with the Simpson compensated type wattmeters is the fact that two terminals are provided for input and two for the output as schematically represented in Figure 5-4. The voltage and current coil connections are internal to the meter.

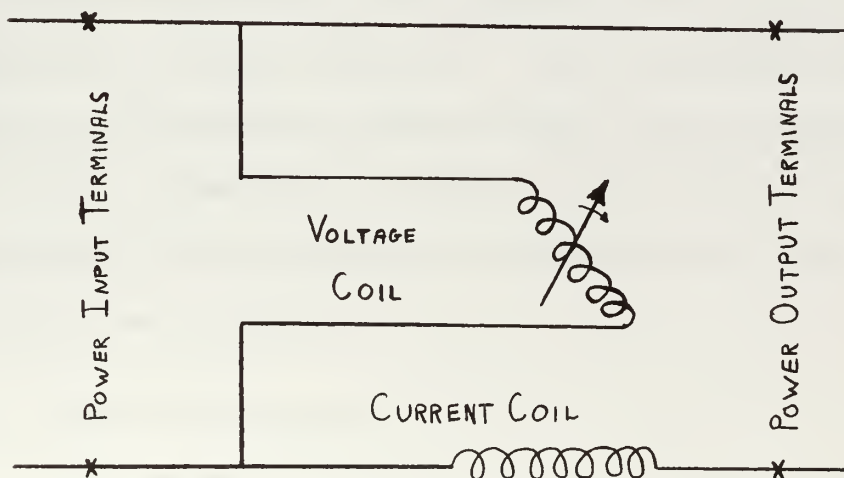


Figure 5-4 Simpson Compensated Wattmeter Schematic Diagram

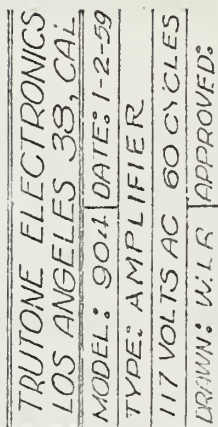
It was necessary to modify the meter so that the voltage and current connections could be made separately. In addition, a further modification to the meter was made so that it would read zero at center scale. In an attempt to make deflection linear and approximately symmetric about this zero, one of the hairsprings to the pointer was removed and reversed. Meter sensitivity was increased to a maximum by removing all series resistance in the current coil circuit, removing all shunts, and insuring that all windings in the respective circuits were connected so as to aid each other.

5.3 Isolation of Tachometer

The voltage coil of the Simpson Wattmeter, as modified, had a resistance of 1470 ohms. This resistance was so low that loading effects upon the tachometer would be most severe. In order to prevent this and to permit selection of different bearing rate sensitivities on the meter an isolating amplifier was located between the tachometer and the bearing rate wattmeter. Unsuccessful attempts to achieve this were made using first an audio amplifier module and then a transistorized audio amplifier. Isolation of the tachometer was finally achieved by using an inexpensive commercial high fidelity audio amplifier. The circuit diagram for this amplifier is shown in Figure 5-5. The volume (gain) control potentiometer was replaced with voltage dividers which were made up of fixed resistors. Selection of different voltage dividers through use of a switch provided for different amplifier gains and hence different bearing rate wattmeter sensitivities.

5.4 Device Test Equipment

Test equipment utilized was the same as that for the initial prototype with the exception of certain additional equipment. This additional equipment consisted of items necessary to generate a constant bearing



49

rate input to the system and to also superimpose a sine wave ripple of variable frequency and amplitude upon this input.

Figure 5-6 shows a diagram of the gear train which was used for generation of a constant bearing rate. The synchro transmitter sending a signal to the servo loop was driven by a permanent magnet d.c. motor through a gear train having a ratio of 42,000 : 1. Letting the synchro transmitter represent the 10 per revolution bearing transmission system, the d.c. motor was then capable of producing a maximum bearing rate of 3 degrees per minute and a minimum ramp of approximately 0.03 degrees per minute. Bearing rates of greater magnitude were available by relocation of the drive motor.

In order to superimpose a sine wave ripple "noise" upon the constant bearing rate input to the servo loop, a Hewlett Packard Low Frequency Function Generator (LFFG), Model 202A, was placed in series with the d.c. power supply which was used to drive the d.c. motor of Figure 5-6. The output impedance of the function generator was such that it completely blocked the d.c. voltage which was to drive the motor. By using the output of the function generator as an input to a General Electric Co. amplidyne, Model 5AM65FB31, and then connecting the output of the amplidyne in series with the d.c. supply to the d.c. motor, generation of a signal having a constant bearing rate and with sine wave ripple superimposed upon it was achieved. A schematic diagram of this is shown in Figure 5-7.

5-5 Testing of Final Prototype Device and Components

In an attempt to determine the gain of the servo amplifier it was discovered that the amplifier had a time constant of approximately 0.4 seconds. It would seem that this time constant would assist in elimination of rapid velocity change. It was determined that this 0.4 second time



BEARING RATE GENERATION
GEAR TRAIN

Note: The numbers by the points of gear contact indicate only the relative numbers of teeth making contact at that point.

Figure 5-6

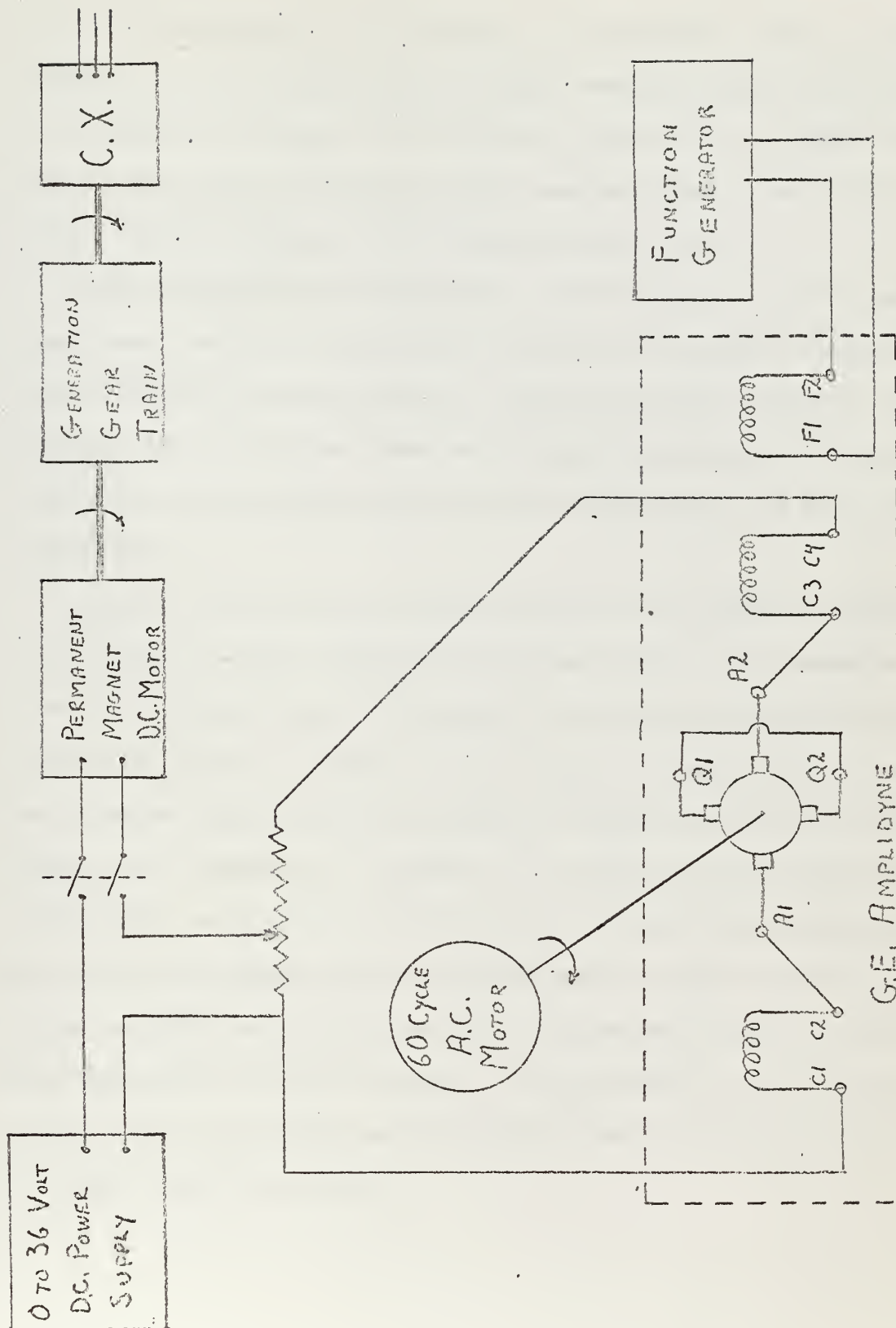


Figure 5-7

BEARING RATE & NOISE GENERATION SYSTEM

constant was the result of the output of the amplifier. The 1.1 megohm resistor, R 6, was removed from the input network of Figure 5-2 in order to eliminate this damping. This was done because with the damping network in the circuit the position servo loop exhibited a stable limit cycle. without damping no limit cycle was experienced.

After elimination of the damping it was discovered that the amplifier itself was a very non-linear device whose gain was somewhat dependent upon the size of the input signal. Because the output waveform of the amplifier was not the same shape as the input no gain curve was obtained. Inability to do this precluded analytical evaluation of the Final Prototype Device.

Table 5-1 lists various bearing rates and noise which were observed to be present at those bearing rates by the author. It is emphasized that these were obtained from observations of continuous bearings of one target as provided by only one sonar set over a period of approximately one hour and therefore these may not necessarily be typical values of noise frequency and/or amplitude. In general, it is very true that high bearing rates exhibit very little noise while lower and lower rates show more and more noise. The maximum noise amplitude (peak to peak) observed was 0.5 degree and had a period of 44 seconds. For the most part noise had peak to peak amplitudes of about 0.3 degree. It was desired to test the Final Prototype Device for accuracy and repeatability with the inputs of Table 5-1 and others which were similar.

BEARING RATE	NOISE PERIOD	NOISE AMPLITUDE (PEAK TO PEAK)	NOISE FREQUENCY	NOISE AMPLITUDE
0	4	.2	.25	.1
1.0	30	.4	.0333	.2
2.3	12	.3	.825	.15
3.8	11	.4	.0911	.2
4.0	15	.4	.0667	.2
6.1	8	.2	.125	.1
6.1	-	0	0	0
7.75	44	.6	.0229	.3
7.8	-	0	0	0
27.5	-	0	0	0

Table 5-1 Typical Bearing Rates and Noise

5.6 Bearing Rate Meter Calibration

The bearing rate wattmeter was mechanically set to midscale zero and then noiseless bearing rates of approximately 0.5, 1.0, 2.0, and 3.0 were used for calibration of the meter face. The output of the tachometer for a bearing rate of 3.0 degrees per minute was amplified by the audio amplifier with a moderate gain. This signal was then impressed across the current coil of the bearing rate meter. The voltage across the voltage and terminals was adjusted by means of a voltage divider so that three deflection to the right were obtained. Maintaining both the voltage across the voltage coil and the gain of the audio amplifier constant calibration of the bearing rate wattmeter face was achieved by determining the bearing rate required to produce a given deflection. Figure 5-8 shows the bearing rate wattmeter face as partially calibrated.

It was intended to obtain an additional calibration scale for very high bearing rates by use of a lower gain on the audio amplifier. Unfortunately the bearing rate wattmeter was ruined before the high bearing rate scale could be calibrated when excessive current was accidentally drawn through the voltage coil.

5.7 Test Results for Final Prototype Device

As previously mentioned, the bearing rate wattmeter burned out while attempting to calibrate the meter. Insufficient time was available before the required date for submission of this to acquire a replacement wattmeter. Because of this testing was incomplete.

However, it can be stated that the device performed very satisfactorily for bearing rates without noise. Results were very repeatable for rates between 0.2 and 4.0 degrees per minute right or left.

Only two bearing rates were tested with noise. In these the effect

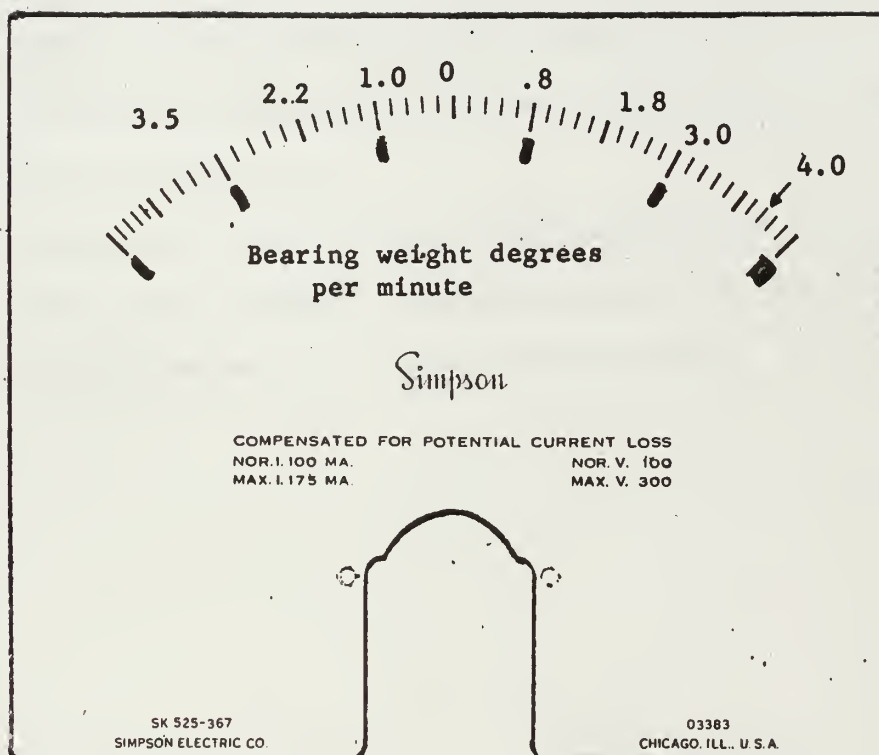


Figure 5-8 Bearing weight wattmeter as partially calibrated

of noise was noticeable but not overpowering. The rates and noise tested were:

(a) 1.0 degree/minute bearing rate with $0.1 (\sin 2\pi (.0333)t)$ noise.

(b) 2.3 degree/minute bearing rate with $0.15 (\sin 2\pi (.825)t)$ noise.

Testing the Final Prototype Device with the above inputs permitted determination of bearing rate to within 0.2 degree per minute in each case. No tests for repeatability were made.

The Final Prototype Device did not entirely meet the specifications set forth in section 2.2.

Calibration of the meter for high bearing rates was not, but could have easily been, achieved. Excellent accuracy would be expected at high bearing rates due to a low signal to noise ratio.

SECTION 6

6. Recommendation for Additional Development and Conclusion

6.1 Recommendation for Additional Development

A very considerable improvement in the minimum bearing rate which could be determined would be expected from an improved gear box using the two motor-generators. Excessive loading of the motor nearest to the control transformer could be prevented by having a clutch mechanism which could disconnect the gearing between that motor and the more "distant" motor. The more "distant" motor would need many more revolutions to cause a given rotation of the control transformer than would the "near" motor.

Use of a motor-generator without any tachometer output at zero velocity would be most desirable.

6.2 Conclusion.

Although the Final Prototype Device did not meet all of the rather stringent requirements placed upon it in section 2.2, it did indicate that use of a servo loop driving a tachometer could be used to obtain bearing rate. As constructed, bearing rates in excess of 2.0 degree per minute is in itself of value to submarines in solving their fire control problem. For this reason additional investigation of this type device is recommended.

BIBLIOGRAPHY

1. United States Naval Postgraduate School, Computer Investigation of a Destroyer Steam Generator, by L. F. Creager, J. D. Fenick, G. H. O'Brien May 1965.
2. Lichenstein, B., Gyros Platforms Accelerometers, Kearfott Division, General Precision, Inc., Little Falls, N. J., June 1963.
3. Savant, C. J., Jr., Control System Design, McGraw-Hill Book Co. Inc., New York, 1958.
4. Thaler, G. J. and Brown, R. G., Analysis and Design of Feedback Control Systems, McGraw-Hill Book Co. Inc., New York, 1958.

APPENDIX A

PROGRAM TOTINER

```

A35=50.355
B48=84.869
C18=7.911
D110=14.964
E46=75.156
F20=11.477
G28=22.933
H16=5.217
SH1=3.743
SH2=2.214
SH3=3.930
SH4=1.560
AXX=0.018595041
BXX=0.003515131
CXX=0.000494315
DXX=0.000069513
EXX=0.056947314
T1=2.60
SY1=3.0
XM1=4.0
X1=(SY1+SH1+B48+A35)*DXX
X2=(C18+SH2+B48)*CXX
X3=(C18+SH3+E46)*BXX
X4=(F20+G28+SH4+D110)*AXX
X5=(T1+H16)*EXX
XNET=X1+X2+X3+X4+X5+XM1
FRICT=2.705*XNET
10 FORMAT(/,8X,3H X1,12X,3H X2,12X,3H X3,12X,3H X4,12X,3H X5,/)
PRINT 10
20 FORMAT(///,5F14.9)
PRINT 20,X1,X2,X3,X4,X5
25 FORMAT(/,5X,24H, TOTAL INERTIA AT MOTOR ,6X,11H, FRICTION ,/)
PRINT 25
26 FORMAT(5X,F20.9,10X,F20.9)
PRINT 26,XNET,FRICT
END
END

```

X1	X2	X3	X4	X5
----	----	----	----	----

.009882455	.046956959	.305805852	.947119818	.445157154
------------	------------	------------	------------	------------

, TOTAL INERTIA AT MOTOR	, FRICTION
--------------------------	------------

5.754922237	15.567064652
TIME, 0 MINUTES AND 12 SECONDS	


```

PROGRAM GEAR 2
A=15.0/110.0
B=20.0/46.0
C=18.0/48.0
D=18.0/48.0
E=28.0/16.0
BX=A*B
CX=A*B*C
DX=A*B*C*D
EX=A*E
AXX=A*A
BXX=BX*BX
CXX=CX*CX
DXX=DX*DX
EXX=EX*EX
21 FORMAT(5F12.9,/)
PRINT 21,A,B,C,D,E
PRINT 21,A,BX,CX,DX,EX
PRINT 21,AXX,BXX,CXX,DXX,EXX
END
END
.136363636 .434782609 .375000000 .375000000 1.750000000
.136363636 .059288538 .022233202 .008337451 .238636364
.018595041 .003515131 .000494315 .000069513 .056947314
TIME, 0 MINUTES AND 8 SECONDS

```


APPENDIX B

Initial Prototype Device

1. Determination of F/J Ratio by Retardation Test

The servo motor was operated with 120 volts, 400 cycles per second on the control and reference phases. These voltages were in phase quadrature. Tachometer excitation of 55 volts, 400 cycles per second was provided. A tachometer RPM vs. tachometer output voltage curve was determined (See Table B-1 and Figure B-1). A recording was made, by photographs, of the oscilloscope display of tachometer voltage vs. time which was produced when the power to the servo motor was secured.

The equation for the motor torque as previously given is:

$$T_M = J \ddot{\theta}_M + F \dot{\theta}_M$$

and

$$\ddot{\theta}_M = \frac{d}{dt} \dot{\theta}_M = \frac{d^2}{dt^2} \theta_M$$

Upon securing the power to the motor

$$T_M = 0$$

$$F \dot{\theta}_M = -J \ddot{\theta}_M$$

$$F/J = - \frac{\ddot{\theta}_M}{\dot{\theta}_M}$$

$$F/J = - \frac{1}{\dot{\theta}_M} \left[\frac{d}{dt} (\dot{\theta}_M) \right]$$

The value of $\frac{d \dot{\theta}_M}{dt}$ may be graphically determined from the slope of the tachometer voltage vs. time oscilloscope trace which was photographed. The value of $\dot{\theta}_M$ may also easily be determined from the amplitude of the trace at the point at which the slope was measured.

Figure B-2 shows the photograph and four tangent lines which were used to determine $\frac{d \dot{\theta}_M}{dt}$.

The values of F/J were determined for each tangent line as follows:

TABLE B-1

TACHOMETER CALIBRATION DATA

RPM SHAFT	TACH OUTPUT	OSCILLOSCOPE FACTOR	TACH OUTPUT (PEAK TO PEAK)	TACH RPM	TACH OUTPUT (RMS)
661	66	1.0	66	3322	23.4
654	65	1.0	65	3290	23.0
645	64	1.0	64	3245	22.6
629	62.7	1.0	6217	3170	22.2
615	61.5	1.0	61.5	3095	21.75
585	58.5	1.0	58.5	2945	20.65
500	50.0	1.0	50.0	2515	17.7
500	100.0	.5	50.0	2515	17.7
475	95	.5	47.5	2390	16.8
448	89	.5	44.5	2255	15.75
420	82.5	.5	41.25	2110	14.6
382	75	.5	37.5	1922	13.25
349	68	.5	34.0	1755	12.05
310	61	.5	30.5	1560	10.78
274	54	.5	27.0	1380	9.55
255	50.5	.5	25.25	1284	8.95
243	96	.25	24.0	1222	8.50
195	76	.25	19.0	972	6.75
136	54	.25	13.5	685	4.78
82	33	.25	8.25	413	2.92
86	34	.25	8.5	432	3.01
45	19	.25	4.75	226.5	1.68

Tach RPM =
RPM Shaft
x $\frac{161}{32}$

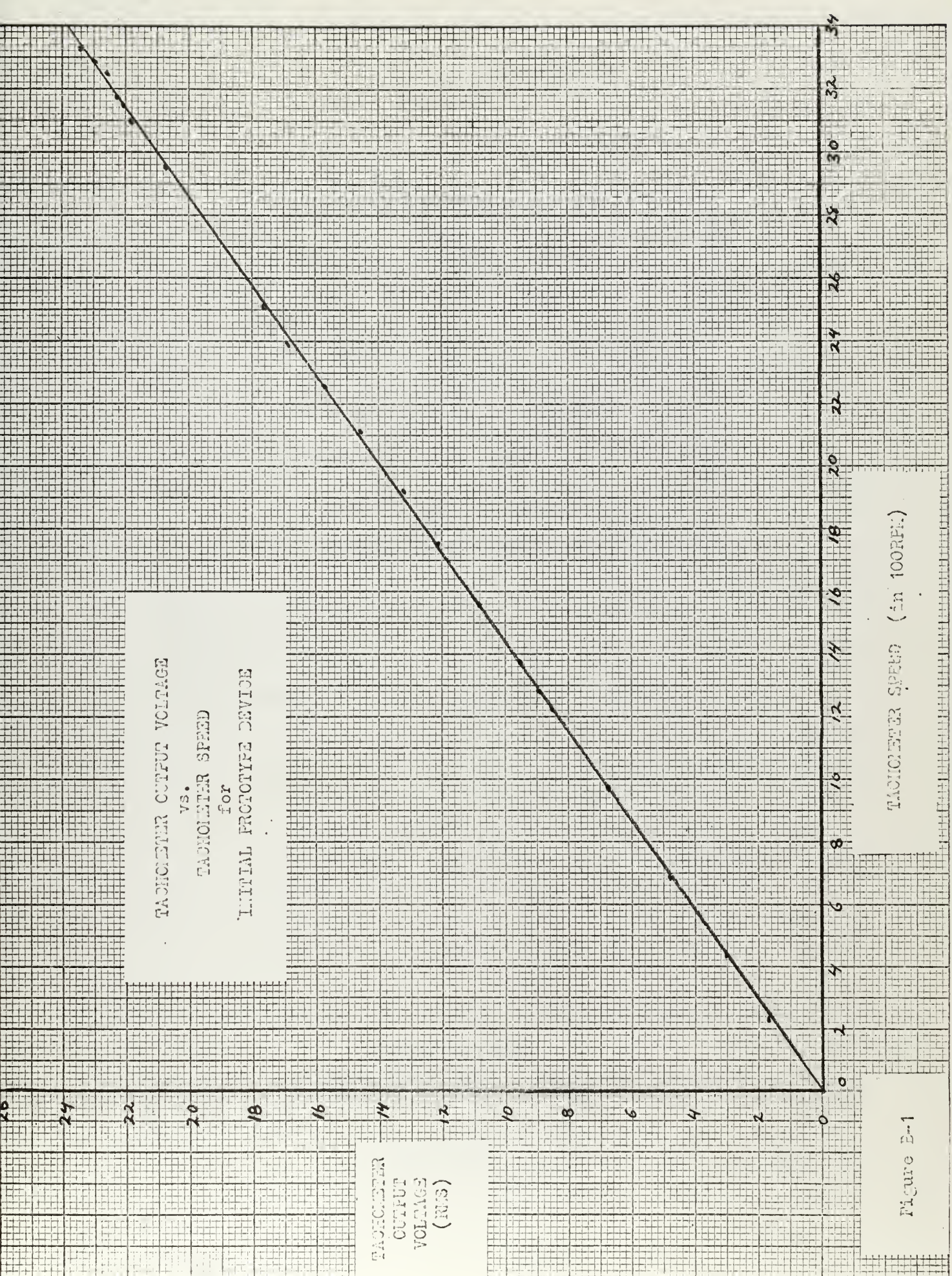
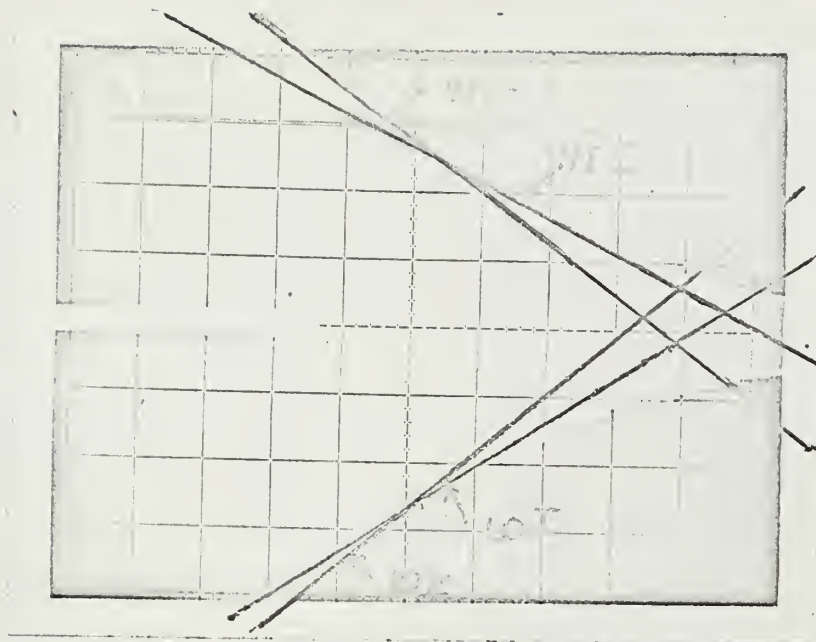


Figure B-1



Tachometer Voltage

Vertical

2.0 volts/cm.

Time (seconds)

Horizontal

0.05 seconds/cm.

RETARDATION TEST
TACHOMETER VOLTAGE vs. TIME

Figure E-2

<u>SLOPE</u>	<u>F/J</u>
Hi I	2.87
Hi II	2.56
Lo I	2.81
Lo II	2.58
<hr/>	
Average F/J	2.705

2. Motor Constants

The servo motor constants $\frac{\partial T_M}{\partial V}$ and $\frac{\partial T_M}{\partial \dot{\theta}_M}$ were evaluated from data supplied by the manufacturer.

$$\frac{\partial T_M}{\partial \dot{\theta}_M} = \left(\frac{2.4 \text{ OZ.-IN.}}{555 \frac{\text{RADIAN}}{\text{SEC.}}} \right) \left(2.54 \frac{\text{CM.}}{\text{IN.}} \right) \left(\frac{1 \text{ POUND}}{16 \text{ OZ}} \right) \left(444,823 \frac{\text{DYNES}}{\text{POUND}} \right)$$

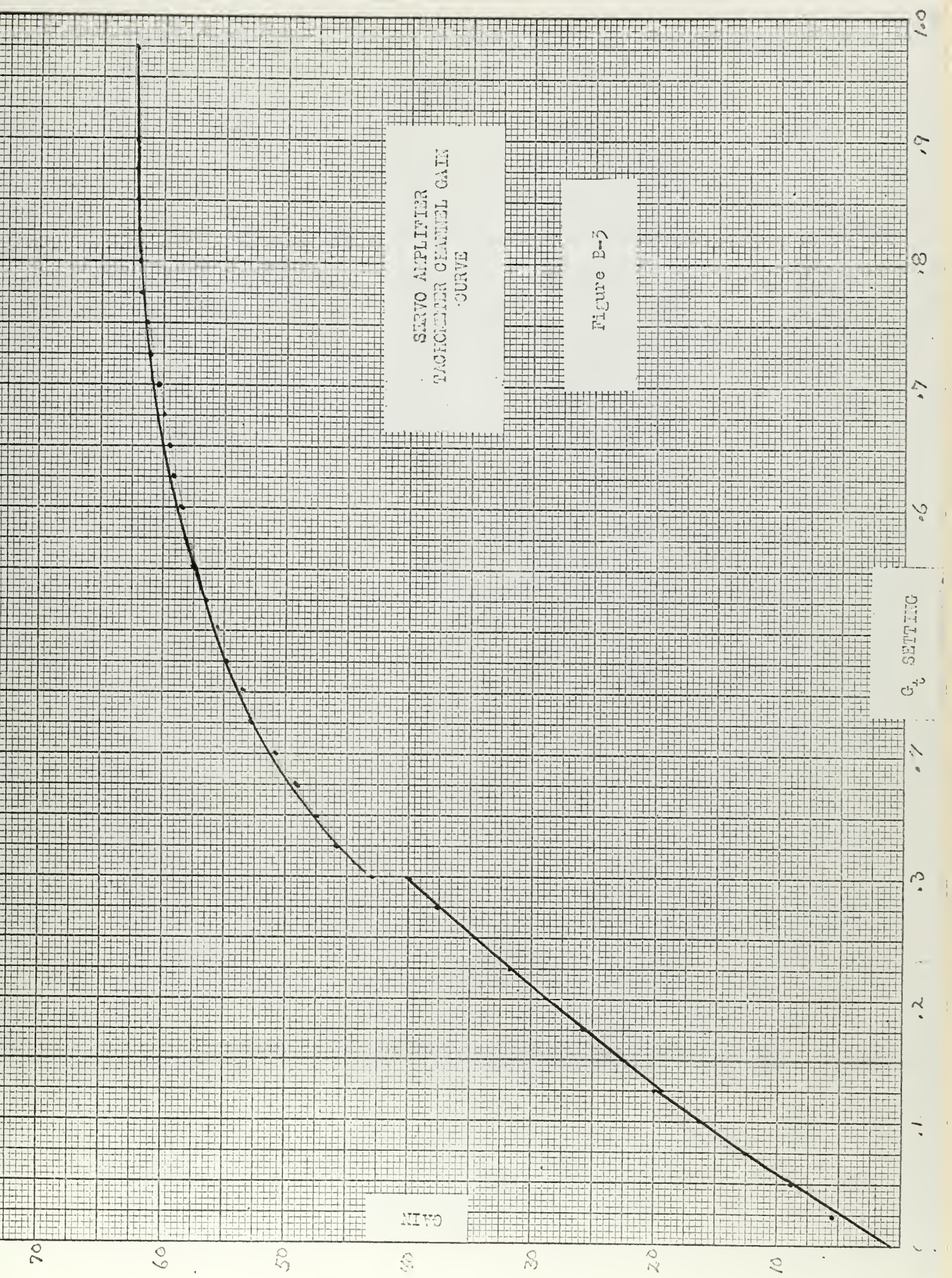
$$\frac{\partial T_M}{\partial \dot{\theta}_M} = 305 \frac{\text{GM.-CM.}^2}{\text{SEC.}} = 305 \frac{\text{DYNE.-CM.}}{\frac{\text{RADIAN}}{\text{SEC.}}}$$

$$\frac{\partial T_M}{\partial V} = \left(\frac{2.4 \text{ OZ.-IN.}}{115 \text{ VOLTS}} \right) \left(2.54 \frac{\text{CM.}}{\text{IN.}} \right) \left(\frac{1 \text{ POUND}}{16 \text{ OZ}} \right) \left(444,823 \frac{\text{DYNES}}{\text{POUND}} \right)$$

$$\frac{\partial T_M}{\partial V} = 1470 \frac{\text{GM.-CM.}^2}{\text{SEC.}^2} = 1470 \frac{\text{DYNE.-CM.}}{\text{VOLT}}$$

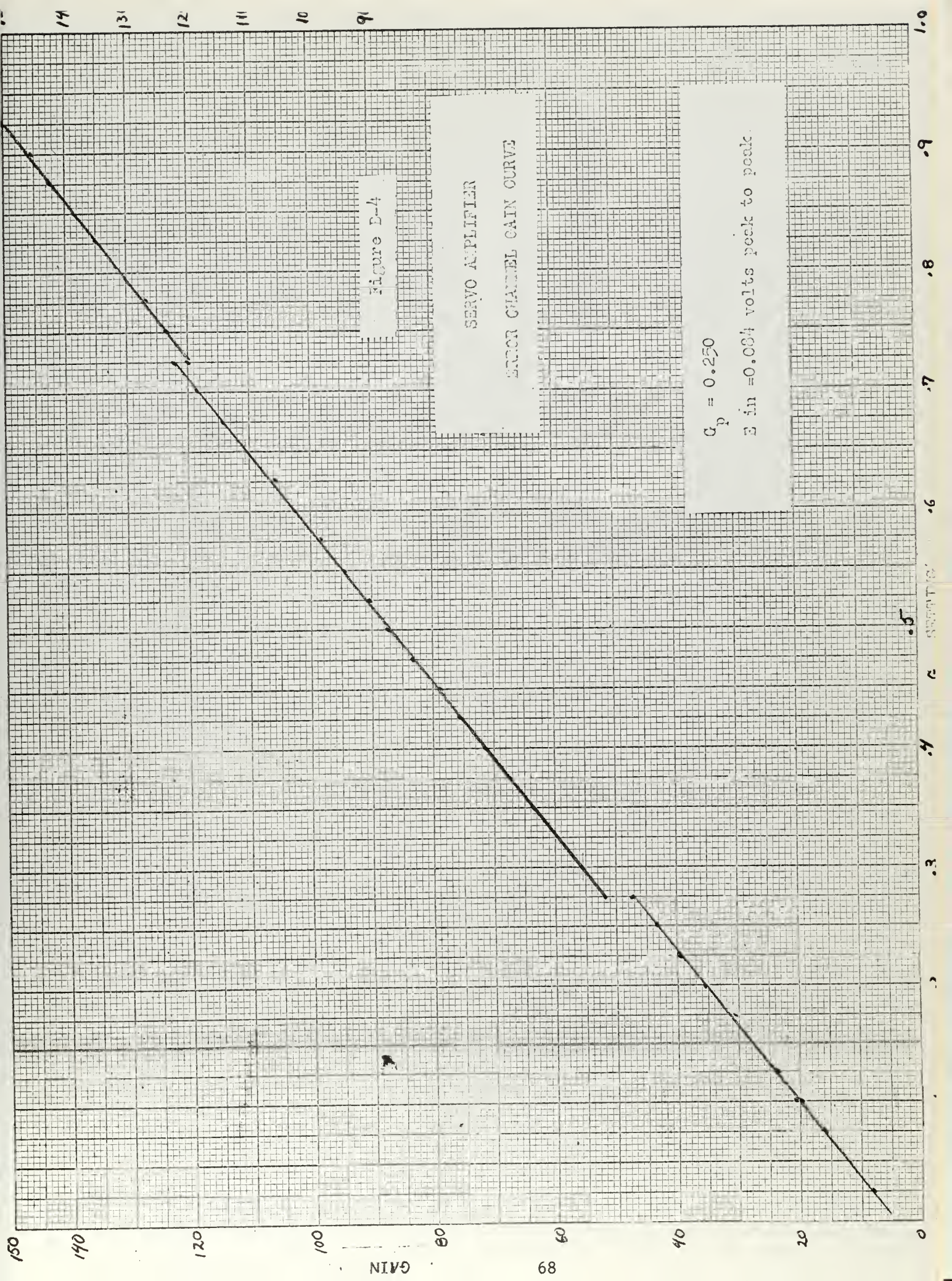
3. Other

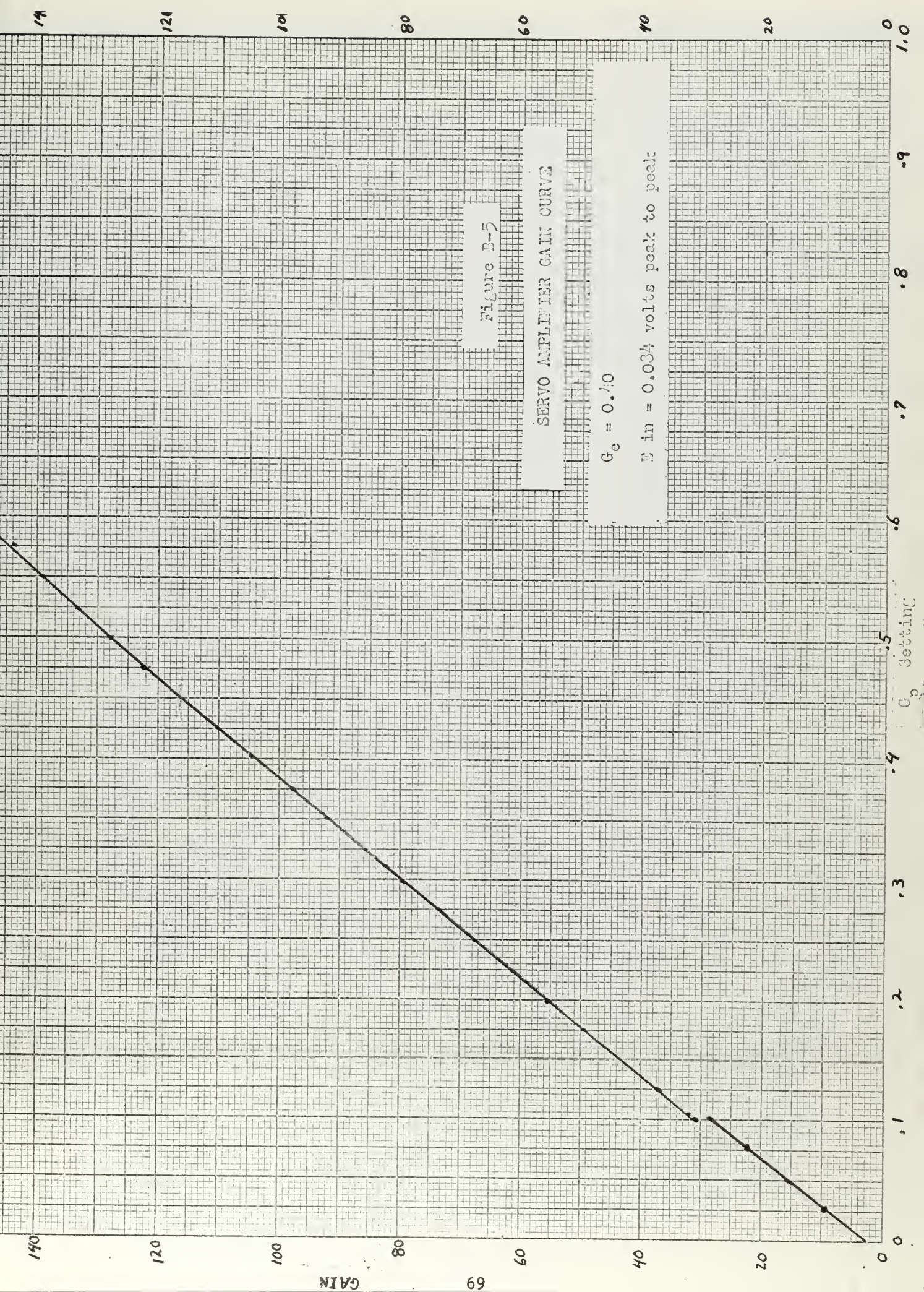
For information purposes only Figures B-3 through B-6 and Tables B-2 through B-5 are provided. These are self explanatory.



SERVO AMPLIFIER
TACHOMETER CHANNEL GAIN
CURVE

Figure B-3





CONTROL TRANSFORMER

SENSITIVITY

CURVE

Figure D-6

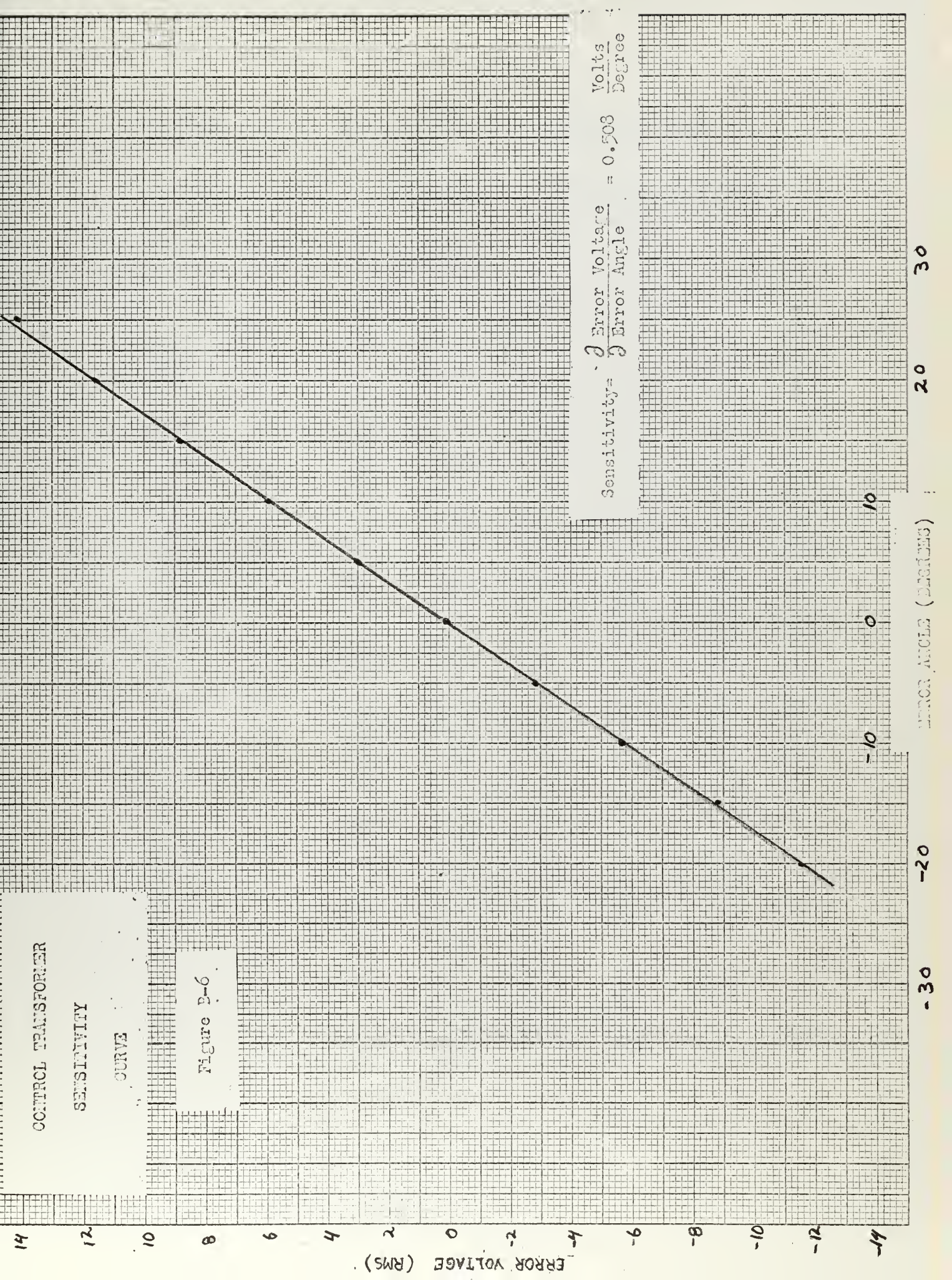


TABLE B-2

TACH CHANNEL GAIN DATA

Gp = .250				Ein = 920 mv peak to peak			
Ge	Ein	Ro	K	Ge	Ein	Ro	K
000	10	8.45	.845	-			
25	10	54.5	5.4	525	10	575	56.5
50	10	88	8.3	50		581	57.5
75	5.0	62.7	12.5	75		585	58.1
100	5.0	81	16.2	600		590	58.5
25	5.0	100	20.0	25		595	59.0
	2.5	48.5	19.4				
50	2.5	56.5	22.4	50		600	59.5
75		64	25.6	75		605	60.0
200		71.5	28.6	700		610	60.5
25		79	31.6	25		614	61.0
50		86.5	34.6	50		617	61.4
75		94.0	37.6	75		618	61.7
300	2.5	100	40	800		-	61.8
	10	450	45				
25	10	460	46	25		-	-
50		475	47.5	50		-	-
75		490	49.0	75		620	-
400		507	50.7	900		-	62.0
25		527	52.7	25		-	-
50		535	53.5	50		624	-
75		547	54.7	75	10	-	62.4
500	10	555	55.5	1000			

TABLE B-5

ERROR CHANNEL GAIN DATA

 $G_n = 250$

Ge	Ein	Eo	K	Ge	Ein	Eo	K
000	8.0	-	-	-	-	-	-
25	8.0	72	9	25	8.0	725	90.6
50	8.0	96	12	50	↑	755	94.4
	5.0	68	15.6	75		767	98.2
75	5.0	80	16.0	600		815	102.0
100	5.0	103	20.6	25		845	105.8
	2.2	45.2	19.7	50		885	110.9
25	↑	52.0	25.6	75		915	114.5
50		60.0	27.5	200	↓	945	118.3
75		69.0	31.4	25	8.0	980	122.8
		77.5	35.2		4.0	480	120.0
25		86.0	39.1	50	↑	495	123.9
50	↓	95.0	43.2	75		505	126.2
	2.2	105	47.7	800		512	128.0
75	8.0	415	51.9	25		540	135.0
300	↑	445	55.6	50		555	138.8
25		475	59.4	75		570	142.5
50		505	63.1	400		585	146.2
75		540	67.5	25		600	150.0
		575	71.9	50		615	153.8
400		605	75.6	75	↓	630	157.5
25		630	78.8	500	8.0	700	161.2
50		650	83.2				
75		665	87.6				

TABLE B-4

AMPLIFIER GAIN DATA

Ge = .400

Ein = 84 mv peak to peak

Gp	Ein	Bo	K	Gp	Ein	Bo	K
000	3.3	8	2.4	-	-	-	-
25	↑	32.5	9.9	525	4.4	585	133.1
50	↑	52	15.8	50	↑	610	138.9
75	↑	73.5	22.3	75	↑	630	145.3
100	3.3	94.5	28.7	600	↑	660	152.2*
100	8.2	256	30.5	25	↑	685	159.9
25	8.2	305	37.2	50	↑	710	161.5
50	↑	355	43.3	75	↑	735	167.1
75	↑	405	49.4	700	↑	760	173.0
200	↑	455	55.5	25	↑	785	178.6
25	↑	505	61.6	50	↑	810	184.2
50	↑	555	67.7	75	↑	835	190.0
75	↑	605	73.8	300	↑	860	195.3
300	↑	655	79.9	25	↑	885	201.6
25	↑	705	86.0	50	↑	905	206.0
50	↑	755	92.1	75	↑	935	212.3
75	↑	800	97.6	900	↑	960	218.3
400	↑	855	104.3	25	↓	985	224.0
25	↑	905	110.4	950	4.4	1010	229.9
50	↑	955	116.5				
75	8.2	1005	122.6				* last plotted point
75	4.4	535	121.8				
500	4.4	560	127.4				

TABLE B-5

CONTROL TRANSFORMER SENSITIVITY

ERROR ANGLE	ERROR VOLTAGE (RMS)
- 20	- 11.6
- 15	- 8.9
- 10	- 5.8
- 5	- 2.9
+ 0	0
+ 5	+ 2.9
+ 10	+ 5.9
+ 15	+ 8.9
+ 20	+ 11.6
+ 25	+ 14.2

$$\frac{\partial \text{Error}}{\partial \theta} \approx \frac{\Delta E}{\Delta \theta} = \frac{(11.6) - (-11.6)}{(+20) - (-20)} = \frac{11.6}{20}$$

$$\frac{\partial \text{Error}}{\partial \theta} \approx .508 \text{ Volts/Degree}$$

thesV345

An investigation into one method of obta



3 2768 001 01370 9
DUDLEY KNOX LIBRARY